An aerial photograph of a wide river, the River Waal and IJssel, showing a large stone weir structure extending across the water. A large blue barge is moving through the water on the right side. The left bank is green with fields and some buildings. The water is a dark greenish-brown color.

DISCHARGE AND LOCATION DEPENDENCY OF CALIBRATED MAIN CHANNEL ROUGHNESS: CASE STUDY ON THE RIVER WAAL AND IJSSEL

Technical report

Author

Boyan Domhof BSc

UNIVERSITY OF TWENTE.

Deltares
Enabling Delta Life 

DISCHARGE AND LOCATION DEPENDENCY OF CALIBRATED MAIN CHANNEL ROUGHNESS: CASE STUDY ON THE RIVER WAAL AND IJSSEL

Technical report

*This report is a part of a graduation research
Adjacent to this report a conference paper has been written*

Delft, Januari 2018

Author

Boyan Domhof BSc

Co-authors

Ir. K.D. Berends (University of Twente)

Dr. ir. A. Spruyt (Deltares)

Dr. J.J. Warmink (University of Twente)

Prof. dr. S.J.M.H. Hulscher (University of Twente)

Abstract

To accurately predict water levels, river models require appropriate description of hydraulic roughness. In most calibration studies of hydrodynamic models the hydraulic roughness coefficient is calibrated because it is the most uncertain parameter (Bates et al., 2004; Hall et al., 2005; Pappenberger et al., 2005; Refsgaard et al., 2006; Vidal et al., 2007; Warmink et al., 2011). The roughness increases as river dunes grow with increasing discharge and is dependent on differences in channel width, bed level and bed sediment. Therefore, we hypothesize that the calibrated main channel roughness coefficient is most sensitive to the discharge and location in longitudinal direction of the river. The calibration study of Warmink et al. (2007) confirms this hypothesis. However, the study of Warmink et al. (2007) does not explain why the calibrated roughness varies along the longitudinal direction of the river and the discharge stages. The main objective in this study is to investigate the location and discharge dependency on the main channel roughness the River Waal and IJssel by calibration. Validation is performed to check if the calibrated roughness also results in accurate water level predictions. The conclusions of this study can be used to improve future calibration studies.

The main channel roughness is calibrated using the Manning roughness formula in the 1D hydrodynamic models of the River Waal for the winters of 1995 and 2011 and IJssel for the winter of 1995 in the Netherlands. The location dependency in the longitudinal direction of the river is modelled using a varying number of roughness trajectories. The discharge dependency is modelled using a varying number of discharge levels. Calibration is performed automatically with the software package OpenDA using the DuD algorithm and a weighted non-linear least squares objective function. Validation is performed using a slightly adapted RMSE criterion.

Results show that the calibrated roughness is mainly sensitive to discharge. Especially the transition from bankfull to flood stage, the effect of the modelled summer dike and the overestimation of bankoverflow in sharp bends are important features to consider in the calibration as it produces better water level predictions. Especially the effect of the modelled summer dike on the calibrated roughness is significant. The optimum number of discharge levels ranges between 4 and 8 discharge levels.

Results of the location dependent calibrated roughness show that incorrect boundary conditions and the modelling of bank overflow in sharp bends greatly influence the roughness. For the Waal, two roughness trajectories of roughly equal length is a found optimum. For the IJssel, three is the optimum found number of roughness trajectories. However, predictions still slightly improve when increasing the number of roughness trajectories in both cases.

Contents

1	Introduction	1
1.1	Background	1
1.2	Objective	1
1.3	Scope	2
1.4	Contributions	2
1.5	Report outline	2
2	Method	3
2.1	Study area	3
2.2	Study cases	5
2.3	Models	6
2.4	Location dependency	7
2.5	Discharge dependency	8
2.6	Calibration method	11
2.7	Performance criteria	11
3	Results: calibration	13
3.1	Location dependency calibrated roughness values	13
3.2	Discharge dependency calibrated roughness-discharge functions	16
4	Results: validation	19
4.1	Location dependency model performance	19
4.2	Discharge dependency model performance	20
5	Discussion	22
6	Conclusion and recommendations	23
6.1	Conclusions	23
6.2	Recommendations	23
	Bibliography	24
A	Method for modelling armoured bed layers and submerged groynes	25
B	Water level frequency distributions	26
C	Calibrated roughness for discharge dependency for Waal 1995 - scenario 1, 2 and 3	27
D	Validation location and discharge dependency combined for Waal 1995	28
E	2D WAQUA 1995 Waal calibration results	29

1 Introduction

1.1 Background

Hydrodynamic river models are used to predict water levels along the river and support decision making in river management. The models are used to monitor the river and to study the effects of measures in the river to decrease the risk of flooding in high water situations and prevent drought in low water situations. Therefore, the model predictions need to be sufficiently accurate. Insufficiently accurate predictions can for example lead to the construction of dikes which are too low which in turn can lead to major damages and casualties in case of flooding.

Hydrodynamic models are calibrated and validated to increase accuracy. Calibration involves minimizing the errors between predicted and observed water levels by altering model parameters for a specific situation. Validation involves verifying if the calibrated model parameters also produce small to no errors between predicted and observed water levels in different situations. In most calibration studies of hydrodynamic models the hydraulic roughness coefficient is calibrated because it is the most uncertain parameter (Bates et al., 2004; Hall et al., 2005; Pappenberger et al., 2005; Refsgaard et al., 2006; Vidal et al., 2007; Warmink et al., 2011). Furthermore, this coefficient is often treated as a dustbin parameter which can compensate for all kinds of model errors, for example simplifying the river bathymetry into a limited number of cross-sections (Morvan et al., 2008 as cited in Warmink, 2011).

Along the longitudinal direction of the river differences in main channel and floodplain width, bed level and bed sediment can for example lead to varying calibrated roughness values. The floodplain vegetation influences the roughness during flood discharge stage. Moreover, as discharge increases, river dunes grow. This in turn increases the bed roughness (Julien et al., 2002). Therefore, it is hypothesized that the calibrated hydraulic roughness is mostly sensitive to discharge and location in longitudinal direction of the river. The calibration study of Warmink et al. (2007) confirms this hypothesis. However, this study does not explain why the calibrated roughness varies along the longitudinal direction of the river and the discharge stages. Our study provides explanations why these variations occur and whether location or discharge dependency is most sensitive. We only focus on the River Waal and IJssel in The Netherlands.

1.2 Objective

The main objective in this study is to investigate the location and discharge dependency on the main channel roughness the River Waal and IJssel by calibration. Validation is performed to check if the calibrated roughness also results in accurate water level predictions. The conclusions of this study can be used to improve future calibration studies. Moreover, Deltares is interested in the conclusions of this study to use in the development of the 6th generation of the national Dutch hydrodynamic river models.

1.3 Scope

In this study we investigate the main channel hydraulic roughness parameters for 1D hydrodynamic river models of large lowland normalized rivers used for water level predictions. The choice for 1D models is based on the shorter calibration times compared to the computational times of 2D (or even 3D) models. We only calibrate the main channel hydraulic roughness parameters. The choice for models of large lowland normalized rivers is based on the availability of and experience with these models at Deltares. The Manning roughness formula is used for the main channel roughness coefficient because it is better suited in the use of compound channels (Huthoff & Augustijn, 2004).

1.4 Contributions

The main part of this study is performed by Boyan Domhof as part of his graduation project. Much input is given by Aukje Spruyt and Koen Berends. Jord Warmink and Suzanne Hulscher independently reviewed the research.

1.5 Report outline

Chapter 2 presents the used method in this study. Next, chapter 3 presents the location and discharge dependent calibrated roughness. Chapter 4 presents the validation of the calibrated roughness found in chapter 3. Finally, chapters 5 and 6 discuss and conclude the results and propose recommendations for further research.

2 Method

2.1 Study area

2.1.1 Waal

The Waal is a tributary of the River Rhine. It is relatively straight and has consistent main channel width which doubles as the river approaches the sea. A schematization of the Waal river model with its observation stations is presented in Figure 2.1. The Waal river starts at river chainage 867 km and ends at 961 km. Note: the river chainage in the models is shorter, namely the river ends at 959.48 km. Figures therefore only present the river chainage from 867 to 959.48 km. The Waal has 7 water level observation stations of which 5 stations can be used in the calibration:

1. Pannerdensch Kop (PK);
2. Nijmegenhaven (NH);
3. Dodewaard (DW) (constructed after 1995);
4. TielWaal (TW);
5. Zaltbommel (ZB);
6. Vuren (Vu);
7. Hardinxveld (HV) (adjusted location of Werkendam in model, cannot be used in calibration because it is the most downstream location).

The Waal has three important features to consider, namely two armoured bed layers and submerged groynes in certain river bends to prevent erosion of the sandy bed in the outer bend. An armoured bed layer is present in the bend near Nijmegen and has been constructed in 1988. In the bend at Sint Andries an armoured bed layer has been constructed too, in 1999. In the bend near Erlecom submerged groynes have been constructed in 1996. These features have a large impact on the roughness and therefore on the water levels. Berends (2013) describes a way to deal with these layers in the calibration of the Waal model, which is summarized in Appendix A.

2.1.2 IJssel

The IJssel is another tributary of the Rhine which is more bendy, has a lower discharge capacity and a slightly lower bed level gradient than the Waal. A schematization of the IJssel model with its observation stations is presented in Figure 2.1. The IJssel river starts at river chainage 878.5 km and ends at 1006 km. Note: the river chainage in the models is shorter, namely the river ends at 996.48 km at Ketel- and Kattendiep. However, as the model has a bifurcation at the downstream boundary to Kattendiep and Keteldiep, we only present the results till the bifurcation. Therefore, the river chainage in the figures ranges from 878.5 to 991.99 km. The IJssel has 12 water level observation stations of which 6 stations can be used in the calibration:

1. IJsselkop (IJK);
2. Westervoort (WV) (constructed after 1995);
3. De Steeg (DeS) (constructed after 1995);
4. Doesburgbrug (DB);
5. Zutphennoord (Zut);
6. Eefebeneden (EB) (constructed after 1995);
7. Deventer (DV) (constructed after 1995);
8. Olst (Olst);
9. Wijhe (Wij) (constructed after 1995);
10. Katerveer (KV);
11. Kampenbovenhaven (KH);
12. Keteldiep/Kattendiep (Kdiep) (cannot be used in calibration because it is the most downstream location).

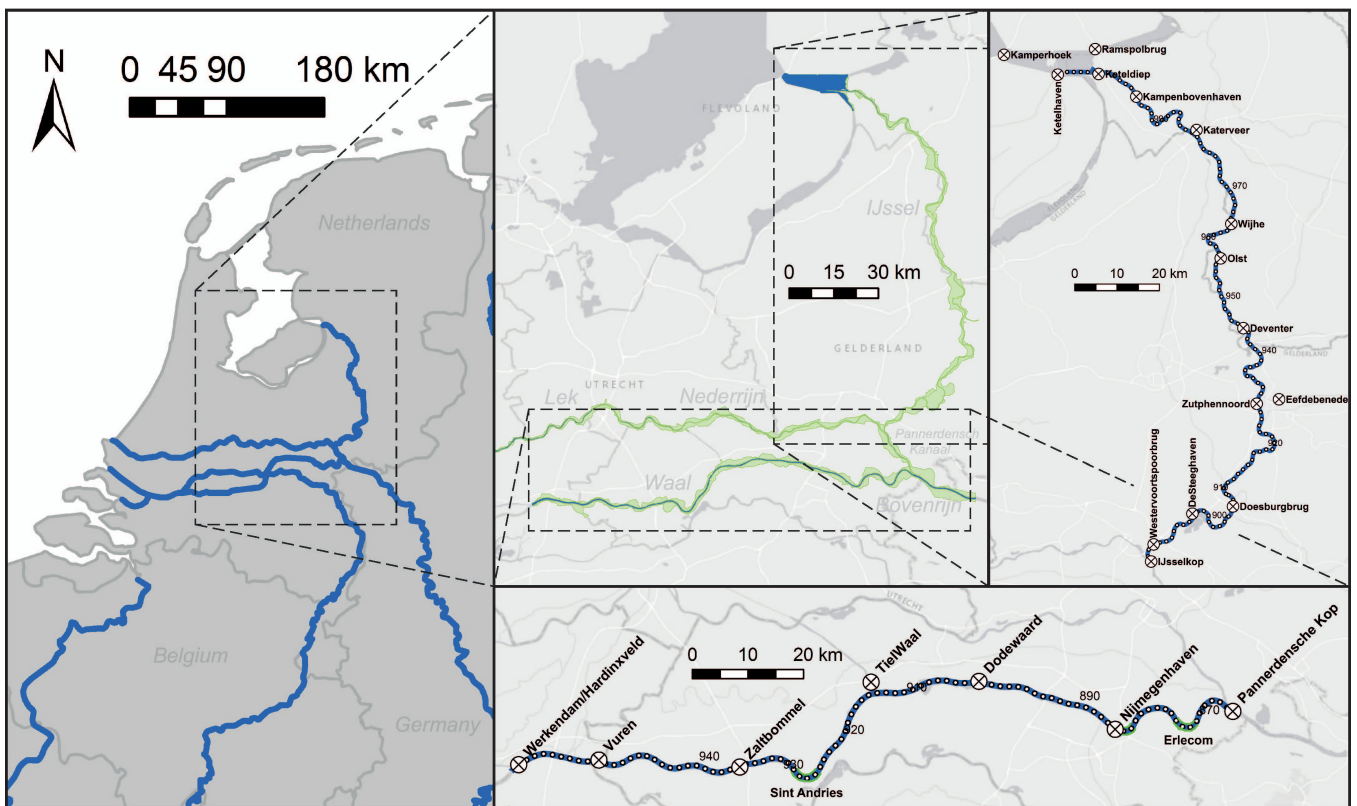


Figure 2.1: Geographic overview of the Waal and IJssel. White dots indicate the river chainage kilometers.

2.2 Study cases

Three study cases are performed:

Waal 1995	Calibration on Waal 1995 model and validation on Waal 1993 and 2011 models
IJssel 1995	Calibration on IJssel 1995 model and validation on IJssel 2011 model
Waal 2011	Calibration on Waal 2011 model and validation on Waal 2015 model

2.2.1 Waal 1995

The discharge wave of 1995 is used for the calibration. This discharge wave is the highest recorded in the Netherlands in recent history and thus provides a large range of discharge levels to calibrate on. The discharge waves of 1993 and 2011 are used for validation. The discharge waves are illustrated in Figure 2.2. The time periods for the three different waves are the following:

1993 (validation)	01/11/1993 00:00 - 31/01/1994 23:00
1995 (calibration)	01/12/1994 00:00 - 28/02/1995 23:00
2011 (validation)	01/11/2010 00:00 - 31/01/2011 23:00

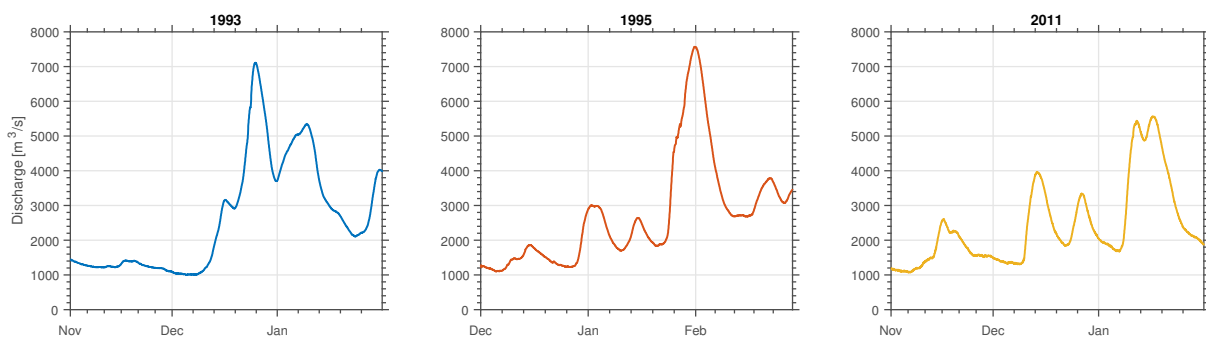


Figure 2.2: Discharge waves of 1993, 1995 and 2011 at Pannerdensch Kop

2.2.2 IJssel 1995

The discharge in the IJssel is a small fraction of the Waal. The discharge wave of 1995 is used for calibration. The discharge waves of 1993 and 2011 are used for validation. The discharge waves are illustrated in Figure 2.3 and the following time periods apply:

1993 (validation)	01/11/1993 00:00 - 31/01/1994 23:00
1995 (calibration)	01/12/1994 00:00 - 28/02/1995 23:00
2011 (validation)	01/11/2010 00:00 - 31/01/2011 23:00

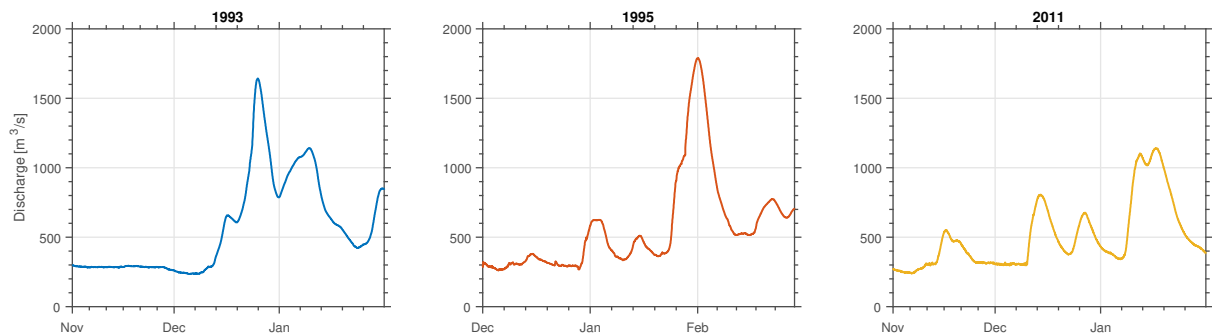


Figure 2.3: Discharge waves of 1993, 1995 and 2011 at IJsselkop

2.2.3 Waal 2011

Both the Waal 2011 and 2015 models are more recent and include some measures of the 'Room for the River'-project (especially the 2015 model). Figure 2.4 presents the discharge waves of 2011 and 2015 of the Waal. The time periods for the two different waves are the following:

2011 (calibration) 01/11/2010 00:00 - 31/01/2011 23:00

2015 (validation) 01/11/2015 00:00 - 31/03/2016 23:00

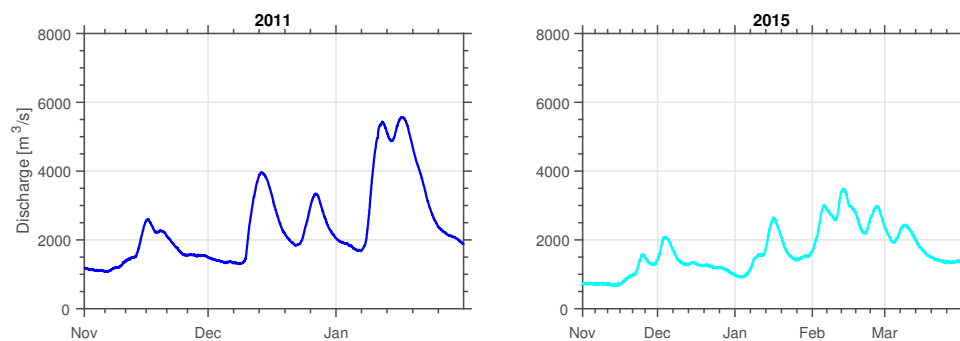


Figure 2.4: Discharge waves of 2011 and 2015 at Pannerdensch Kop

Note: the discharge wave data of 2015 at Pannerdensch Kop has not been corrected for volumetric differences as was done for the 1993, 1995 and 2011 discharge waves.

2.3 Models

Four different versions of the Dutch Rhine-model (of which the Waal and IJssel are part) are used following the presented study cases:

1. j93_5-v4 (1993)
2. j95_5-v4 (1995)
3. j11_5-v3 (2011)
4. j15_5-v2 (2015)

Both the 1993 and 1995 models are practically the same except for the boundary data. The 2011 and 2015 models differ on more points. This is due to the natural and man-made changes in the river (i.e. 'Room for the River'-projects) during the years between 1995 and 2011/2015. Though, the main discretization of the models is the same. All the available models are made using the hydrodynamic modelling program SOBEK 3 and the WAQ2PROF method.

2.4 Location dependency

To investigate the location dependency of the main channel roughness, three different situations (of which the Waal 1995 calibration is illustrated in Figure 2.5) are calibrated:

1. Whole time-period of discharge wave;
2. Discharge level in bankfull stage;
3. Discharge level in flood stage.

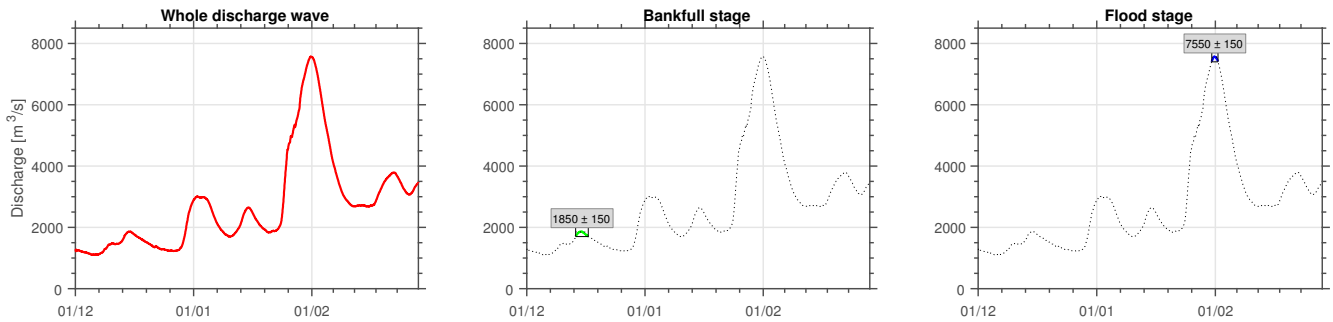


Figure 2.5: Three calibration cases illustrated: using 1) whole discharge wave, 2) a discharge level of 1850 ± 150 m^3/s on only the first and lowest discharge peak (bankfull stage) and 3) a discharge level of 7550 ± 150 m^3/s on only the fourth and highest discharge peak (flood stage)

Note: Because the discharge wave in the IJssel greatly changes as it progresses more downstream (i.e. due to diffusion of the wave and large lateral discharge sources like the Twentekanaal), the discharge levels are changed in size and height according to the progression of the wave.

2.4.1 Calibration routine

All the observation data are taken into account in the calibration, because we want to capture as much of the river behaviour as possible. The roughness trajectory configuration for N number of trajectories is presented in Table 2.1. The trajectory lengths are roughly of equal length. Otherwise, no calibration takes place indicated by n.a. in the table.

Note: Also calibrations on 2D WAQUA results, used as a representation of the observation data, were performed for the Waal 1995 case. In these calibrations we could increase the number of roughness trajectories above the number of existing roughness trajectories. However, these calibration proved to be unsuccessful as the calibrated 1D model was too similar to the 2D model.

Table 2.1: Roughness trajectory configuration for varying number of trajectories and for the Waal 1995, IJssel 1995 and Waal 2011 cases

N traj.	Waal 1995	IJssel 1995	Waal 2011
1	PK-HV	IJK-Kdiep	PK-HV
2	PK-TW, TW-HV	IJK-Olst, Olst-Kdiep	PK-TW, TW-HV
3	n.a.	IJK-Zut, Zut-KV, KV-Kdiep	PK-DW, DW-ZB, ZB-HV
4	PK-NH, NH-TW, TW-ZB, ZB-HV	n.a.	n.a.
5	PK-NH, NH-TW, TW-ZB, ZB-Vu, Vu-HV	IJK-DB, DB-Zut, Zut-Olst, Olst-KV, KV-Kdiep	PK-NH, NH-DW, DW-TW, TW-ZB, ZB-HV
6	n.a.	IJK-DB, DB-Zut, Zut-Olst, Olst-KV, KV-KH, KH-Kdiep	PK-NH, NH-DW, DW-TW, TW-ZB, ZB-Vu, Vu-HV

2.5 Discharge dependency

In each calibration case the five (Waal 1995) or six (IJssel 1995 and Waal 2011) existing roughness trajectories are calibrated with a varying number of discharge levels. Four scenarios are distinguished in applying discharge levels:

Scenario 1: peaks	Based on discharge peaks
Scenario 2: valleys	Based on discharge valleys
Scenario 3: peaks and valleys	Based on both discharge peaks and valleys
Scenario 4: robust method	Based on dividing the discharge wave in N equally-spaced discharge levels

We refer to scenarios 1, 2 and 3 as the method with discharge levels which are more or less determined by a constant discharge for a longer period of time, "constant discharge levels method". It ensures that the calibration is focused on one discharge value without being dominated by the water level errors due to the "rising" and "falling" parts (i.e. steep incline/decline before/after the peak/valley) of the discharge wave. Calibration scenarios 1, 2 and 3 are not performed for the IJssel 1995 and Waal 2011 cases.

Scenarios 1, 2 and 3, however, largely depend on subjective choices (e.g. which peaks and valleys are to be calibrated, which discharge wave is going to be used, how big is the window around the discharge levels). To avoid making these choices and therefore have a more objective method, we present a robust method where the discharge wave is divided into N equal-spaced discharge levels, from (roughly) the minimum to the maximum discharge of the wave, which are calibrated in one run. In this case, two choices remain, namely which discharge wave and how many discharge levels are to be used in calibration. We refer to this scenario as the "robust method" as this method can be applied to any discharge wave irrespectively of the shape, length and height of the discharge wave. The discharge dependency calibrations of the IJssel 1995 and Waal 2011 are only performed with the robust method.

2.5.1 Scenario 1-3: Constant discharge levels method

Discharge levels

Figure 2.6 illustrates scenarios 1, 2 and 3 for the Waal 1995 calibration. In the figure only the color-highlighted parts of the discharge wave are calibrated. Each discharge level is placed roughly on the bottom of the valley or top of the peak with a standard window of $150 \text{ m}^3/\text{s}$. The latter means there is a bandwidth of plus and minus $150 \text{ m}^3/\text{s}$ around the set discharge level. When the discharge windows of peaks or valleys overlap, they are defined as one level, as, for example, can be seen for level $1750 \pm 150 \text{ m}^3/\text{s}$ in the second subplot of the figure.

Calibration routine

The three scenarios are calibrated using a standard calibration procedure, as illustrated in Figure 2.7. In this procedure, we start with calibrating the lowest discharge level and move up to the highest discharge level. The choice of starting with the lowest discharge level is because at this point it is in the bankfull stage. Therefore, only the effects of the main channel are calibrated into the main channel roughness. Table 2.2 presents the levels which are calibrated for N number of discharge levels for each of three scenarios. The calibration procedure is as follows (and graphically illustrated in Figure 2.7):

2 levels The lowest discharge level is calibrated first. The roughness is modelled as a constant roughness. The initial roughness of all five trajectories is set at $n = 0.03 \text{ s/m}^{1/3}$. Next, the calibrated

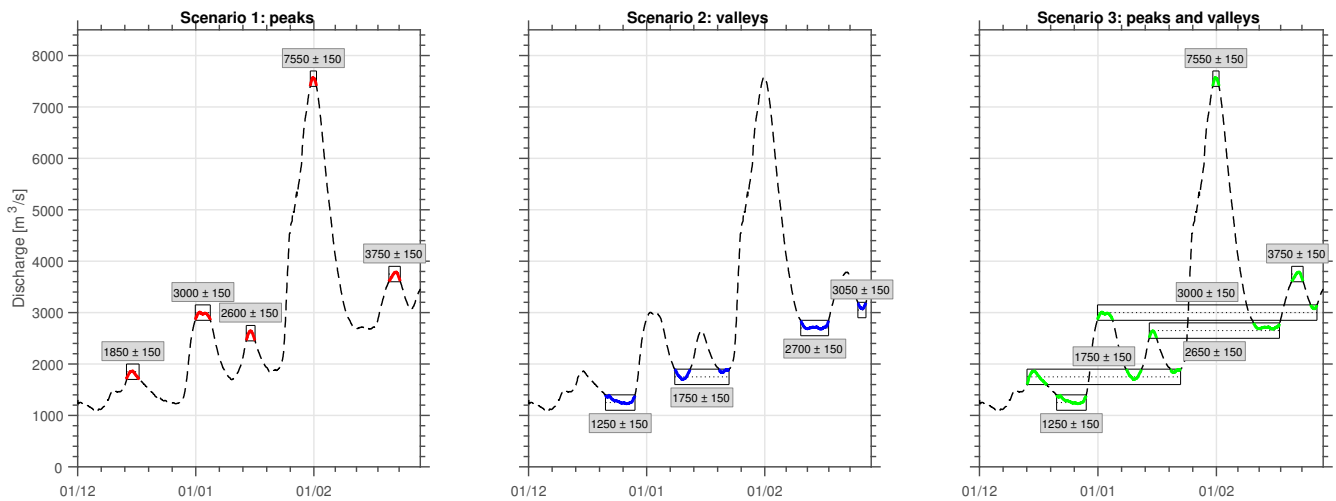


Figure 2.6: Scenarios 1, 2 and 3 illustrated on the 1995 discharge wave

Table 2.2: Discharge levels which are calibrated for N number of discharge levels for scenario 1, 2 and 3 for Waal 1995 calibration

# of levels	Scenario 1: peaks	Scenario 2: valleys	Scenario 3: peaks and valleys
2	Q1850 Q7550	Q1250 Q3050	Q1250 Q7550
3	Q1850 Q3000 Q7550	Q1250 Q2700 Q3050	Q1250 Q2650 Q7550
4	Q1850 Q2600 Q3750 Q7550	Q1250 Q1750 Q2700 Q3050	Q1250 Q2650 Q3750 Q7550
5	Q1850 Q2600 Q3000 Q3750 Q7550	n.a.	n.a.
6	n.a.	n.a.	Q1250 Q1750 Q2650 Q3000 Q3750 Q7550

roughness of the lowest discharge level is used as the initial roughness for the roughness calibration of the highest discharge level. This will result in a linear roughness-discharge relation.

$N > 2$ **levels** In the next step, the roughness discharge function, obtained in the previous two levels calibration case, is used as the initial roughness estimation. Depending on the N number of levels, we interpolate the initial roughness for the given discharge level height on this linear roughness discharge function. Next, we calibrate the roughness starting with the second lowest discharge level. After that, we calibrate the next lowest discharge level, till we have calibrated the highest discharge level as the last level.

2.5.2 Scenario 4: Robust method

Discharge levels

Scenario 4 involves using the robust method which has minimal (subjective) choices to be made and can be used for any discharge wave. The discharge wave is divided into N equal-spaced discharge levels from (roughly) the minimum to (roughly) the maximum discharge of the wave with $N = [2, 3, 4, 6, 8, 12]$. For $N = 2$ the minimum and maximum discharge (thus 1000 and 8000 m³/s) are chosen as the two levels for calibrating a discharge-roughness function. For $N > 2$ discharge levels are added equal-spaced in between the minimum and maximum discharge with the minimum and maximum discharge as fixed endpoints. Table 2.3 shows the minimum and maximum discharge level for three cases. The tidal influence downstream of the Waal is incorporated in these levels.

Calibration procedure for 4 levels, scenario 2: valleys

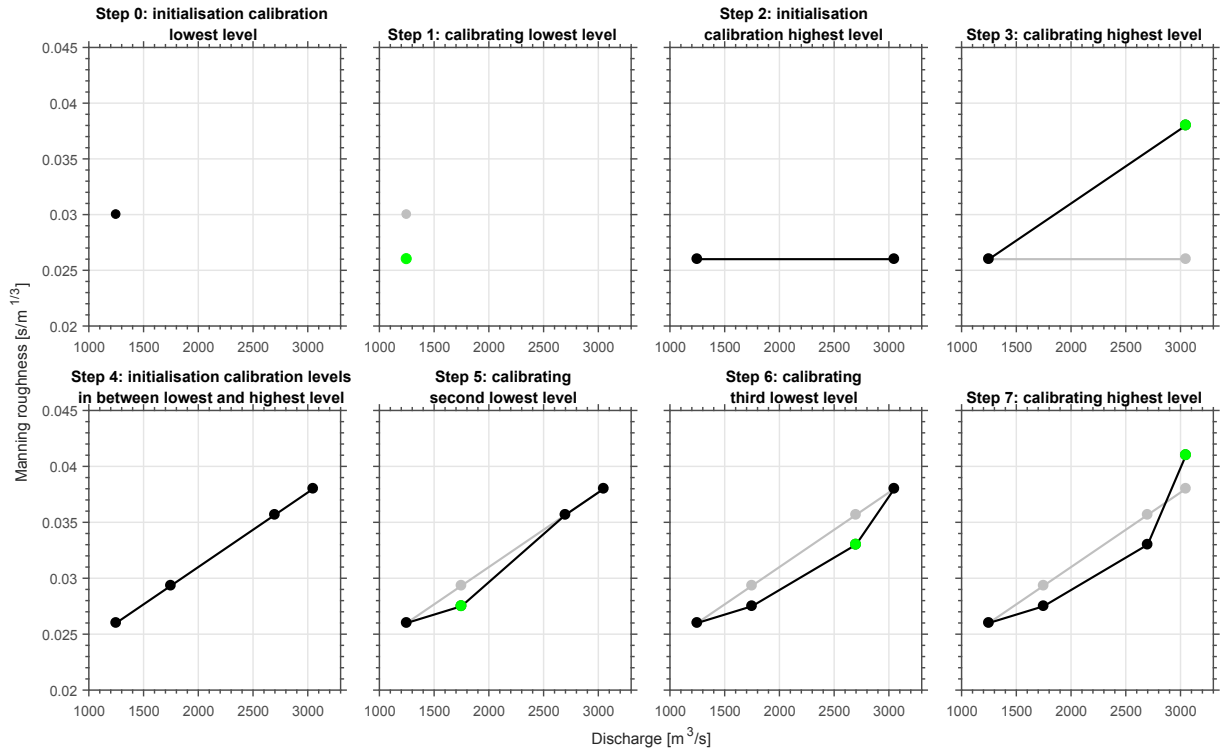


Figure 2.7: Example of the calibration procedure, illustrated using 4 discharge levels for scenario 2: valleys on the Waal 1995 discharge wave. A green dot indicates a newly calibrated discharge level.

Table 2.3: Minimum and maximum discharge levels (in m^3/s) for robust method for Waal 1995, IJssel 1995 and Waal 2011 cases

Case	Minimum	Maximum
Waal 1995	1000	8000
IJssel 1995	200	1900
Waal 2011	750	600

Calibration routine

OpenDA provides the ability to calibrate all the discharge levels in one calibration run. During this "everything-at-once"-run we calibrate on the whole time period of the discharge wave. Due to this approach it is expected that OpenDA needs more iterations to find a solution for the calibration problem. Therefore, the maximum number of outer iterations N_1 is increased to 100 and the maximum number of inner iterations N_2 to 10 compared to the standard calibration options as presented in Table 2.4.

First for $N = 2$, both the levels at the minimum and maximum are calibrated in one run using the standard initial roughness of $n = 0.03 \text{ s/m}^{1/3}$. For $N > 2$, we first generate an initial estimate of the roughness by interpolating the result of the $N = 2$ calibration. After this has been done, the "everything-at-once"-approach is again applied.

2.6 Calibration method

OpenDA (OpenDA, 2015) is used to calibrate the 1D hydrodynamic models using a weighted non-linear least squares objective function and the DuD-algorithm (Ralston & Jennrich, 1978). The standard calibration options are stated in Table 2.4. The calibration is based on water levels. Windows around a discharge level can be used to limit the time period of the water level data to be used in calibration (e.g. only calibrating the top of a discharge peak). The initial roughness before calibration is set at Manning $0.03 \text{ s/m}^{1/3}$ corresponding to a sandy dune bed (Julien, 2002). In each calibration case, the trajectory roughness is determined as uniform along the whole trajectory. Finally, the first three days of the discharge wave are not taken into account for the calibration to remove any remaining model initialization errors.

2.7 Performance criteria

We choose to use the Root Mean Square Error (RMSE) function to evaluate the performance of the model in the calibration and validation cases due to the mathematical similarity with the used objective function (i.e. weighted nonlinear least squares [as shown in Table 2.4]) in OpenDA:

$$RMSE = \sqrt{\frac{1}{k \cdot l} \sum_{i=1}^k \sum_{j=1}^l \gamma_{i,j} \cdot (y_{i,j} - \hat{y}_{i,j})^2} \quad (2.1)$$

with y denoting the simulated water levels, \hat{y} denoting the observed water levels, γ denoting a weighting factor, l denoting the number of observed water levels of one observation location and k denoting the number of observation stations. In case of $k = 1$, only the RMSE of one observation station is calculated. When multiple observation stations are taken into account, thus $k > 1$, the number of l observed water levels should be equal for all k observation stations to ensure each residual weighs equally in the calculated RMSE. The first three days of water level data is discarded following the same choice in the calibration.

The weighting factor γ is used to account for the more frequent low water levels and less frequent high water levels (as illustrated Appendix B). When no weighting is applied to account for this, the water levels for the daily normal discharge will dominate over the high water levels during peak discharges in the calculated RMSE. The weighting factor is determined per observation station and per year by dividing an uniform distribution with the frequency distribution of the observed water levels. The bin size of the frequency distribution is determined using the Freedman-Diaconis rule (as summarized in Izenman (1991)). The water level frequency distributions for each of the four used discharge waves are illustrated in Figure ??.

Table 2.4: Calibration options that are used in this study. $y_{i,j}$ denotes the observed water level and $\hat{y}_{i,j}(\theta)$ the simulated water level for a given time j with i the number of time instances, a given observation location i with k the number of locations and θ denoting a set of calibration parameters.

	Description	Formula	Value	Notes
Calibration algorithm	DuD (Doesn't use Derivatives)			The choice of the DuD calibration algorithm is based on its robustness and efficiency on non-linear functions (e.g. large-scale 1D hydrodynamic river models) and converges the quickest in comparison to the simplex and Powell's method (Schwanenberg et al., 2011; Post, 2012; Mulder, 2014).
	Objective function	Weighted nonlinear least squares $Q(\theta)$	$Q(\theta) = \frac{1}{2} \sum_{i=1}^k \sum_{j=1}^l W_i (y_{i,j} - \hat{y}_{i,j}(\theta))^2$	$W_i = 1/\sigma_i^2$ with σ_i the measurement uncertainty of each observation station which is equal to 0.01 m for each observation station in the Waal and IJssel
Stopping criteria	Maximum number of outer iterations N_1		20	An outer iteration is part of the calibration routine.
	Maximum number of outer iterations N_2		5	An outer iteration is part of the calibration routine.
	Maximum absolute objective difference T_1		1.0	
	Maximum relative objective difference T_2		0.0001	
	Maximum relative linearized objective difference T_3		0.00001	
	Maximum relative step-size in linesearch T_4		10.0	Stepsize in linesearch is part of the calibration routine
	Maximum absolute average residual at all locations T_5	$\frac{1}{m} \left \sum_{i=j}^m (y_{i,j} - \hat{y}_{i,j}(\theta)) \right < T_5 \quad \forall i$	0.005	Is equal to 5 mm of residual waterdepth

3 Results: calibration

3.1 Location dependency calibrated roughness values

Figures 3.1, 3.2 and 3.3 show the calibrated roughness for the Waal 1995, IJssel 1995 and Waal 2011 models for a varying number of roughness trajectories. Overall, the calibrated values are fairly constant along the whole river length. More large deviations in calibrated roughness values between the three different cases (i.e. whole discharge wave, bankfull and flood discharge level) occur at the downstream boundary. This can be attributed to an insufficiently correct boundary condition. The backwater effect occurring because of the boundary condition does not predict the water levels correctly at the observation stations influenced by the backwater effect. The calibration compensates for this by adjusting the roughness. For the Waal models, the roughness is lowered for the bankfull stage and increased for the flood stage. This effect is not present in the IJssel model, where the roughness at the downstream boundary is roughly the same for both bankfull and flood stage cases. The difference in roughness for the Waal models can be attributed to a changing backwater (i.e. from an M1 to an M2 curve (Chow, 1959, p.226)). In the Waal models a roughness increase at Dodewaard/TielWaal (between 901 and 933 km) can be seen. It is unknown why this happens.

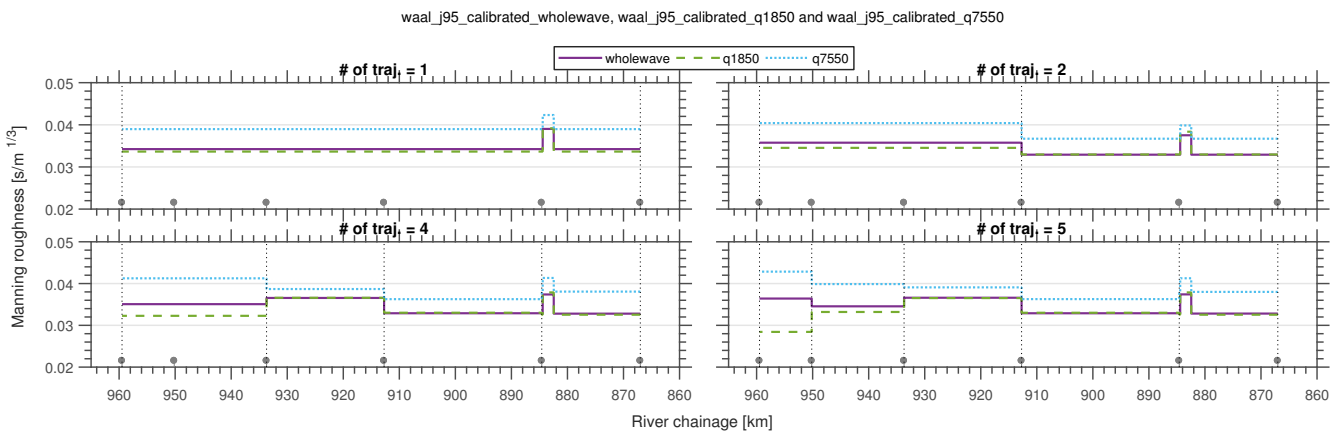


Figure 3.1: Calibrated roughness of the Waal for whole discharge wave, with a 1850 m³/s discharge level (bankfull stage) and with a 7550 m³/s discharge level (flood stage) for 1995 discharge wave for varying number of roughness trajectories. Dotted black lines show the division into N number of trajectories, grey dots above x-axis show the observation locations. The small roughness increase around 883 km is due to the armoured bed layer at Nijmegen

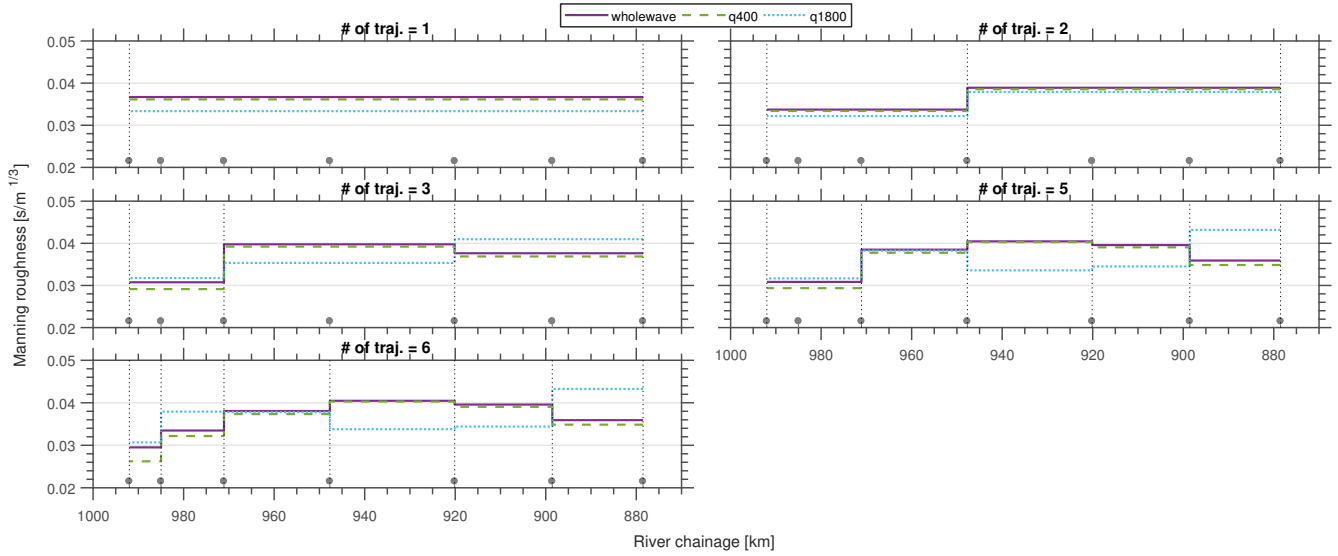


Figure 3.2: Calibrated roughness of the IJssel for whole discharge wave, with a $400 \text{ m}^3/\text{s}$ discharge level (bankfull stage) and with a $1800 \text{ m}^3/\text{s}$ discharge level (flood stage) for 1995 discharge wave for varying number of roughness trajectories. Dotted black lines show the division into N number of trajectories, grey dots above x-axis show the observation locations

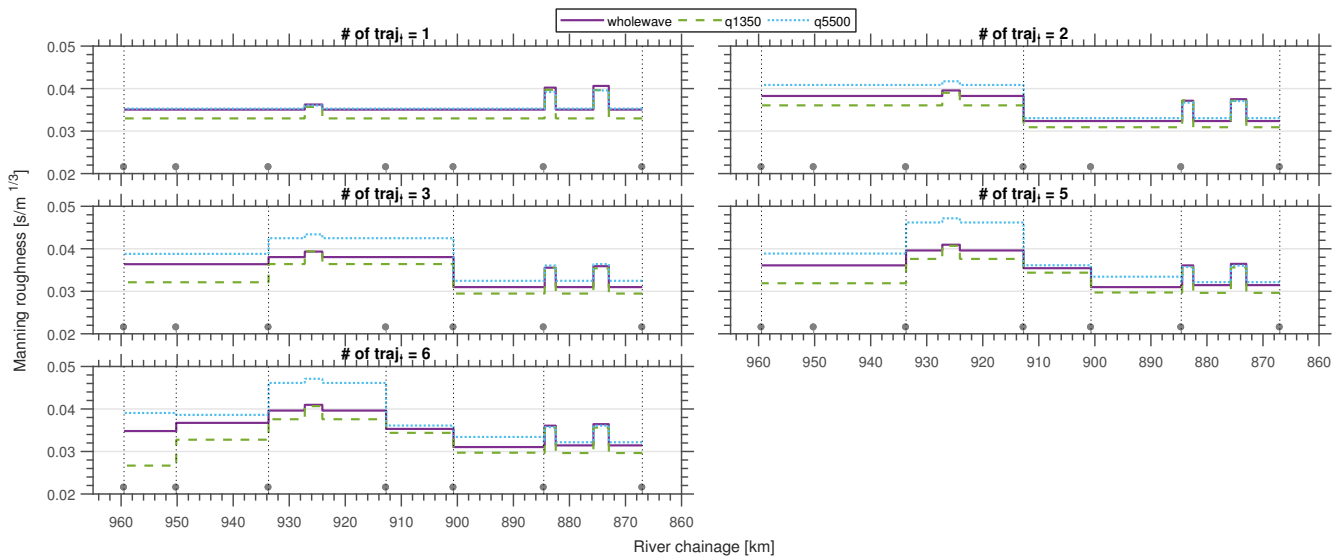


Figure 3.3: Calibrated roughness of the Waal for whole discharge wave, with a $1350 \text{ m}^3/\text{s}$ discharge level (bankfull stage) and with a $5500 \text{ m}^3/\text{s}$ discharge level (flood stage) for 2011 discharge wave for varying number of roughness trajectories. Dotted black lines show the division into N number of trajectories, grey dots above x-axis show the observation locations. The small roughness increases around 874, 883 and 926 km are due to respectively the submerged groynes at Erlecom and the armoured bed layers at Nijmegen and Sint Andries

The sudden "dive" in the calibrated roughness for the IJssel model at trajectories Doesburgbrug-Zutphennoord (from 899 to 920 km) and Zutphennoord-Olst (from 920 to 943 km) for the flood stage is caused by an incorrect model representation in the bends. Large bends are present near the observation stations where the "dive" occurs (i.e. Doesburgbrug [899 km], Zuthpennoord [920 km] and Olst [943 km]). Normally, during a flood the water will overflow the bends, seeking the easiest way to flow. However, this process is difficult to model in 1D. Therefore, large overestimation of the water level occurs at these points as illustrated in Figure 3.4. The 1D model representation tries to solve this problem with

large cross-sectional profile with large storage areas in the bends (illustrated in Figure 3.5), but this is insufficient. The calibration then ultimately solves this problem by lowering the roughness.

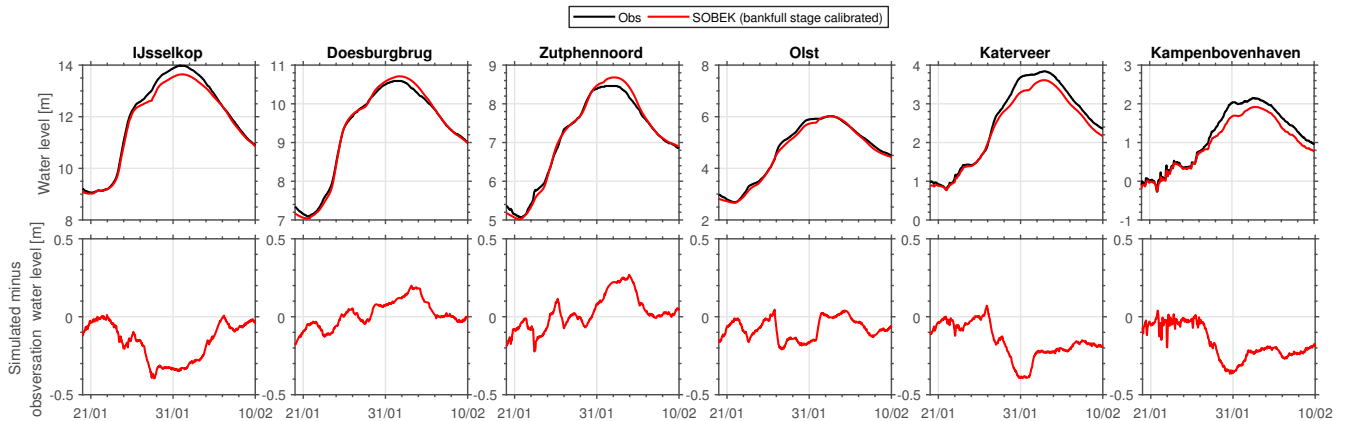


Figure 3.4: Water level overestimation in the bends of the IJssel for the flood stage of 1995. The water levels are largely overestimated at Doesburgbrug and Zutphennoord. The water level at Olst is not under- or overestimated



Figure 3.5: 1D schematization of the IJssel bend at the Rhederlaag near Doesburgbrug compared to the actual floodplain width. Red line indicates main channel, grey lines perpendicular to main channel indicate size of 1D cross-sectional profiles

3.2 Discharge dependency calibrated roughness-discharge functions

Only the robust method results (i.e. scenario 4) are considered here. The calibrated roughness of scenarios 1, 2 and 3 for the Waal can be found in Appendix C. A calibration with the robust method for the 2D WAQUA 1995 Waal model is performed too using six discharge levels. These calibration results can be found in Appendix E.

Figures 3.6, 3.7 and 3.8 show the calibrated roughness-discharge functions for a varying number of roughness trajectories. The roughness functions for all three models show overall increasing roughness with discharge. This is not true for the trajectories DB-Zut and Zut-Olst for the IJssel model due to overestimation of the water levels in the river bends (see previous section for more information). When adding more discharge levels, more details in the roughness-discharge functions appear. The most prominent details are the roughness increase at lower discharges after which a roughness decrease occurs to finally end in a roughness peak at higher discharges.

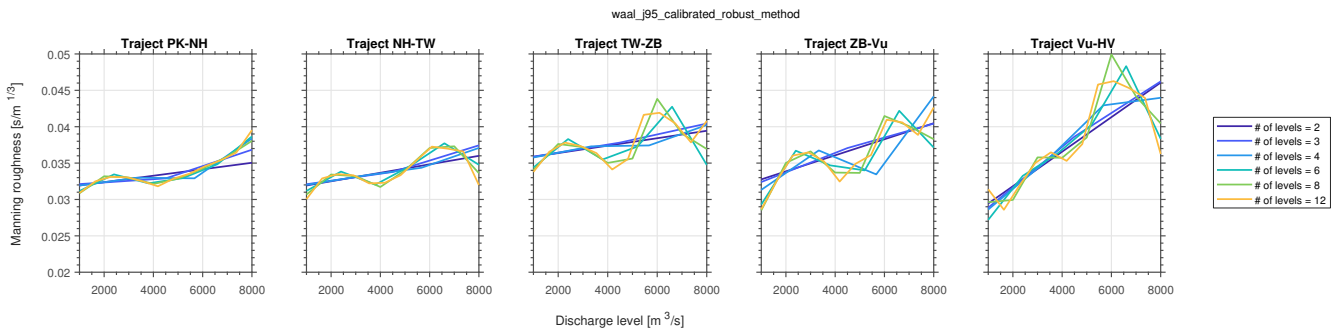


Figure 3.6: Calibrated roughness-discharge functions of the Waal for 1995 discharge wave for varying number of discharge levels based on the robust method

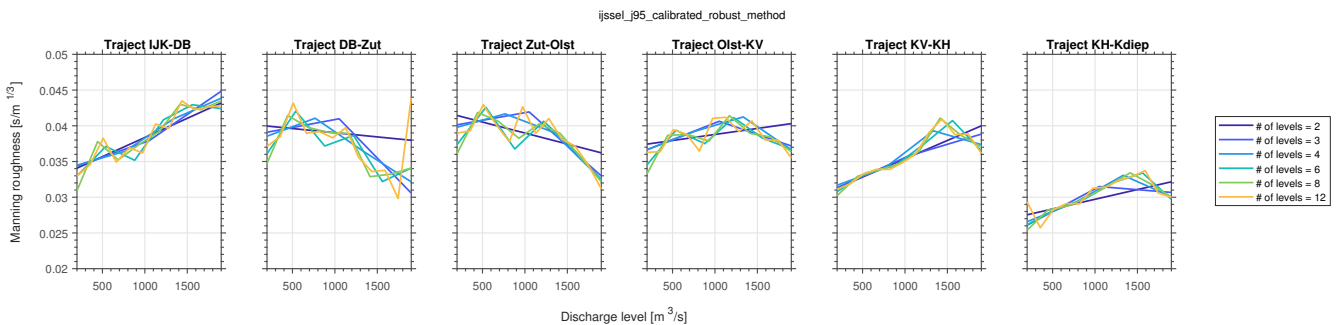


Figure 3.7: Calibrated roughness-discharge functions of the IJssel for 1995 discharge wave for varying number of discharge levels based on the robust method

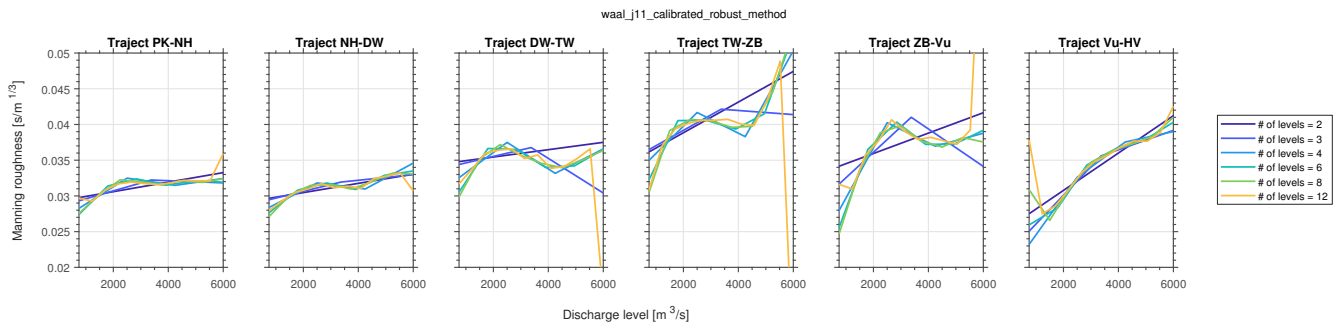


Figure 3.8: Calibrated roughness-discharge functions of the Waal for 2011 discharge wave for varying number of discharge levels based on the robust method

The roughness increase at lower discharges can be attributed to the growth of river dunes. As these bedforms grow, the roughness also grows (Julien et al., 2002; Wilbers & Ten Brinke, 2003). This growth could also explain why the calibrated roughness increases overall with discharge.

The roughness decrease around 4000 m³/s for the Waal and 800 m³/s for the IJssel after the increase can be attributed to the transition from bankfull to flood stage. When the water level starts to flow into the floodplain, the total wetted perimeter suddenly increases whereas the total wetted area remains fairly constant. This results in a sudden decrease in the hydraulic radius and this in turn leads to a lower compound roughness (see Figure 3.9). However, as the calibrated roughness still decreases, it is assumed that the lowering of the compound roughness is not sufficient enough to accurately predict the water level at that stage. The discharge at which this transition occurs depends on the roughness at lower discharges. A high roughness at lower discharges results in a higher water level which in turn leads to a more early flow into the floodplain.

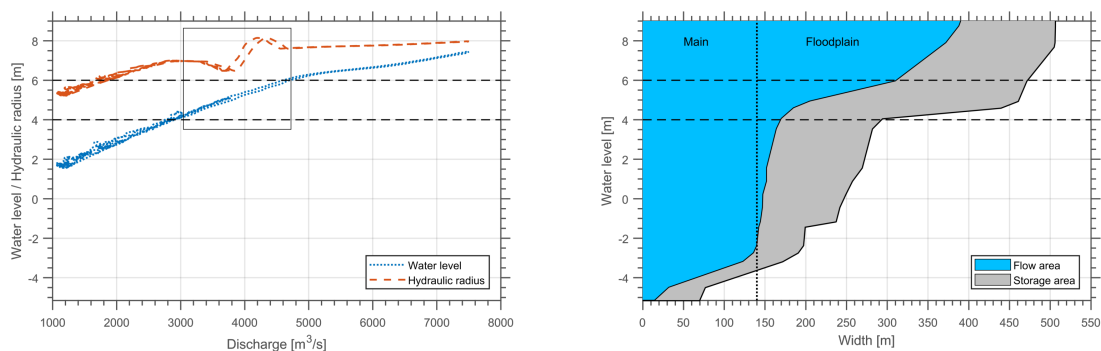


Figure 3.9: Water level and hydraulic radius as a function of the discharge at Zaltbommel for 2 discharge levels. The cross-sectional profile is plotted too. The box in the left plot indicate the drop and recovery of the total hydraulic radius

The roughness peak at higher discharges is a direct result of the modelled summer dike. In the used models a summer dike option is present, a feature of the SOBEK 3 modelling program. The summer dike option is a modelling trick to capture the effect of the actual summer dike in a 1D model, which is normally not possible due to the nature of 1D. As increasingly more water volume is stored behind the summer dike more downstream, a discrepancy between the observed and predicted water levels starts to grow. In reality, openings are opened in the summer dike during high discharge peaks. Therefore, the floodplain is already inundated when the water level has not yet reached the crest level of the summer dike. Figure 3.10 illustrates this discrepancy.

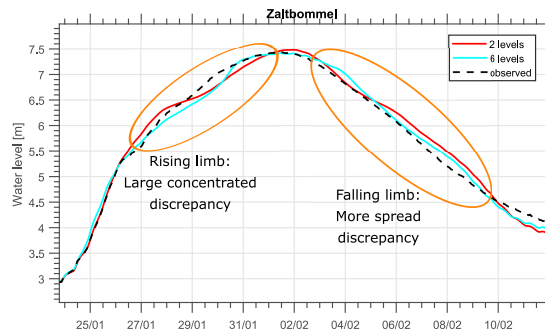


Figure 3.10: Predicted and observed water level at Zaltbommel. Discrepancy between predicted and observed water level is more concentrated on rising limb for 2 levels. Roughness increase at 6 levels minimizes total discrepancy for both rising and falling limb

The discrepancy is centered around one specific discharge due to the way the overflow over the summer dike is modelled (Deltares, 2015, p.90). A discrepancy on the falling limb of the discharge peak also starts to form but across the whole range of the peak. This is also a result of how the flow of the stored water behind the summer dike back into the main channel is modelled. In the end, we see a large discrepancy on the rising limb of the discharge peak for a specific discharge whereas a more spread out discrepancy on the falling limb of the peak occurs. The calibration favors the larger discrepancy on the rising limb over the more spread out discrepancy on the falling limb and ultimately increases the roughness at a specific discharge level to minimize the total error between predicted and observed water levels. The roughness peak is less apparent in the calibrated roughness of the Waal 2011 model because multiple moderately high discharge peaks occur in this discharge wave leading to a more spread out calibration result.

During the investigation of the effect of the modelled summer dike, we found that the flow area of the modelled summer dike is in most cross-sections in the used models higher than the total area. These areas are calculated by the WAQ2PROF method. Physically a larger flow area than the total area is not possible but SOBEK ignores this by calculating the effect of the flow and total area separately. Therefore, the flow area is mostly overestimated leading to a very high roughness peak. Although calibration solves this problem, still it is not ideal. A calibration is performed with six discharge levels on the Waal 1995 model where the flow area is manually limited to the total area. Furthermore, a calibration without the modelled summer dike is performed too. Figure 3.11 shows the calibrated roughness-functions of these two calibrations compared to the case without adjustment to the modelled summer dike. The figure shows that the modelled summer dike has a very large impact on the calibrated roughness at higher discharges. It is advised to investigate how this impact translates to the accuracy of the predicted water levels.

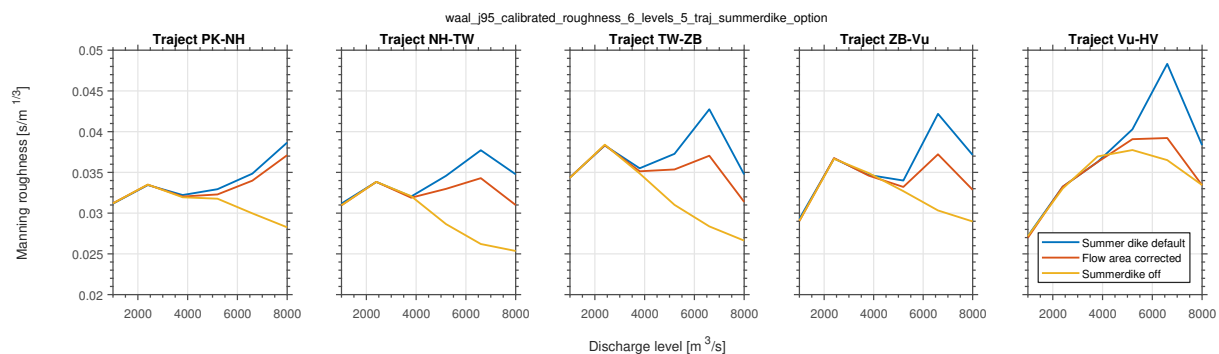


Figure 3.11: Effect of the modelled summer dike on the calibrated roughness-discharge functions with six discharge levels

4 Results: validation

4.1 Location dependency model performance

Figures 4.1, 4.2 and 4.3 present the validation of the calibration on the Waal 1995, IJssel 1995 and Waal 2011 models for a varying number of roughness trajectories. All validation cases show the worst model performance when calibrating on a discharge level in the flood stage (i.e. highest discharge peak). This is because only during the highest discharge peak the water levels get simulated correctly. When calibrating on a discharge level in the bankfull stage (i.e. lowest discharge peak or deepest discharge valley), then model performance is much better. However, taken the whole discharge wave into account in the calibration proves to generate the best overall model performance. This is because the model performance is more sensitive to the used discharge levels as the big difference in RMSE values between the bankfull and flood stage shows.

For the Waal, both the validation of the calibration on 1995 and 2011 show an optimum number of roughness trajectories around two. This corresponds to an average trajectory length of 45 km. For the IJssel an optimum is visible in the validation around three trajectories, which corresponds to an average trajectory length of 40 km. However, as the figures also show, the performance still increases after the optima. This shows that the existing number of roughness trajectories used in both river models is good enough.

It is important to note that the calculated RMSE for the Waal 1995 model validation using 2011 in the whole discharge wave and bankfull discharge level cases is dominated by the errors induced at observation locations TielWaal and Zaltbommel. There is reason to believe that these errors are a result of better bed level measurements using multibeam in 2011 compared to the single beam measurements in 1995. A quick analysis indeed showed a difference in bed level between these two years around TielWaal. However, these results are too preliminary to be conclusive.

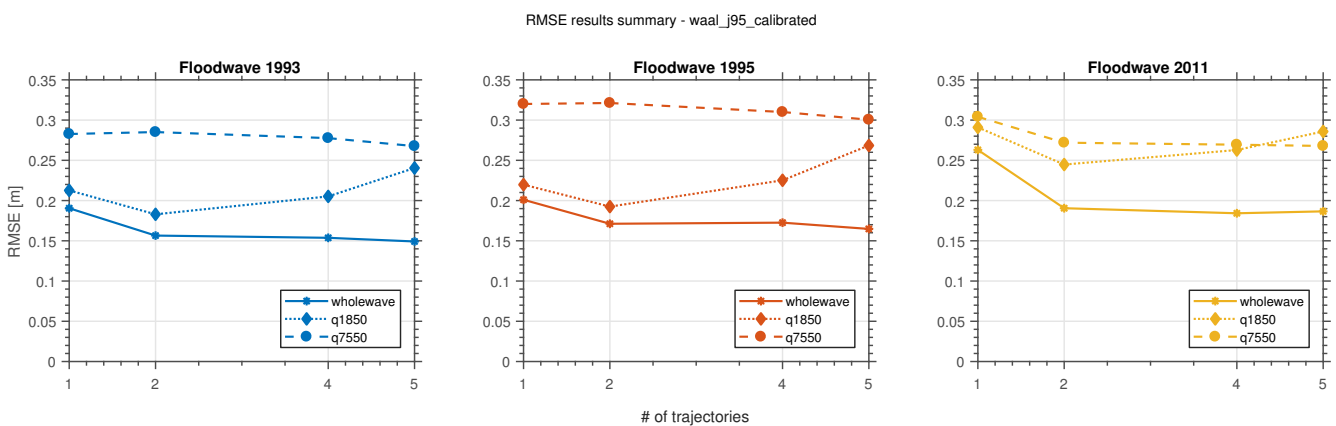


Figure 4.1: RMSE based on the whole discharge wave for 1993, 1995 and 2011, for varying number of roughness trajectories, calibrated on whole discharge wave, a bankfull stage discharge level and a flood stage discharge level and 1995 Waal discharge wave

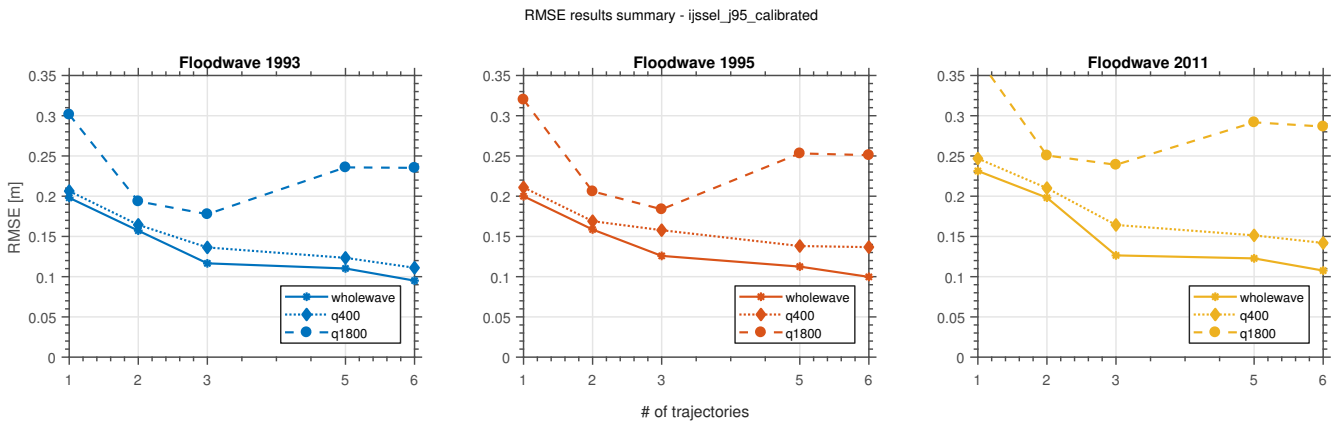


Figure 4.2: RMSE based on the whole discharge wave for 1995 and 2011, for varying number of roughness trajectories, calibrated on whole discharge wave, a bankfull stage discharge level and a flood stage discharge level and 1995 IJssel discharge wave

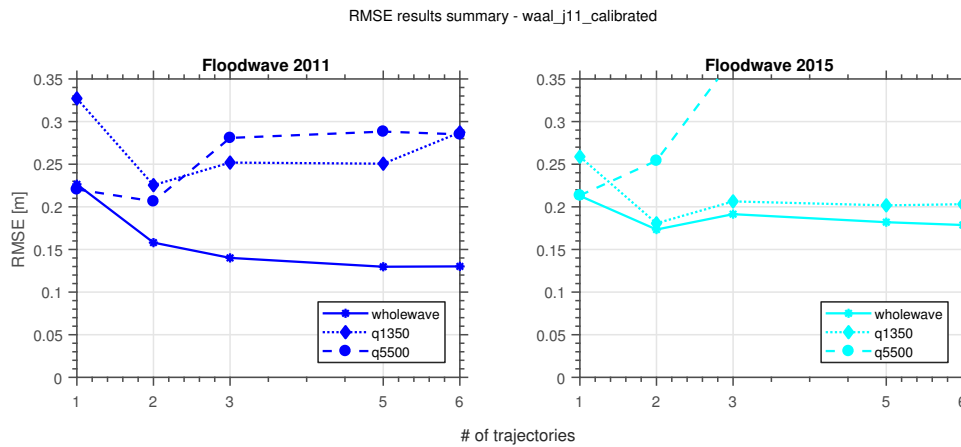


Figure 4.3: RMSE based on the whole discharge wave for 2011 and 2015, for varying number of roughness trajectories, calibrated on whole discharge wave, a bankfull stage discharge level and a flood stage discharge level and 2011 Waal discharge wave

4.2 Discharge dependency model performance

Figures 4.4, 4.5 and 4.6 present the validation of the calibration on the Waal 1995, IJssel 1995 and Waal 2011 models for a varying number of discharge levels. Compared to varying the number of roughness trajectories, these results show a much better model performance (as expected from the previous chapter). When making the roughness a function of the discharge with only two discharge levels, the RMSE in some cases is already better than the lowest found RMSE in the location dependency cases. This proves that model performance is more sensitive to the discharge than to location.

The validation results of the calibration on the Waal 1995 model are mixed. When looking at the 1993 validation, the first, third and fourth scenario produce equally well model performance, though at different number of discharge levels. The results of the 2011 validation, however, show the lowest calculated RMSE for the second and third scenario. However, it is of interest to have good model performance at both validation cases. Based on this, only the third and fourth scenario produce the best model performance at around six discharge levels.

The validation results of the calibration on the IJssel 1995 and Waal 2011 models show more or less the same results. The IJssel validation shows that four discharge levels produce the best results and the Waal validation six or eight discharge levels.

Looking back at the calibrated roughness-discharge functions in Chapter 3, these optimum of four to eight discharge levels correspond to roughness-discharge functions where the transition from bankfull to flood stage and the effect of the summer dike is present. Therefore it is advised to adjust existing calibration methods to capture these effects as it proves to result in better model performance.

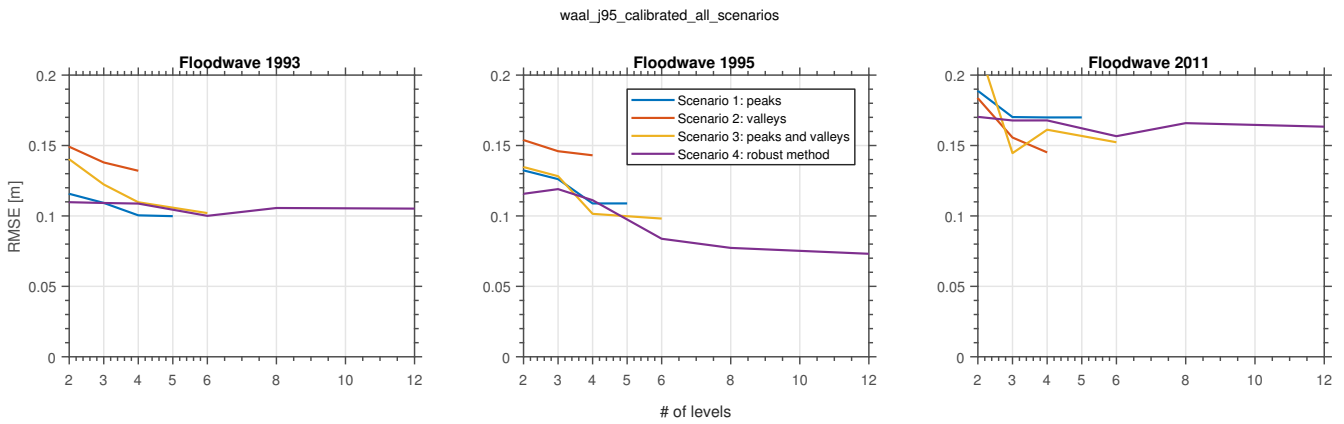


Figure 4.4: RMSE based on the whole discharge wave for 1993, 1995 and 2011 and for varying number of discharge levels based on peaks, valleys, peaks and valleys and the robust method and 1995 Waal discharge wave

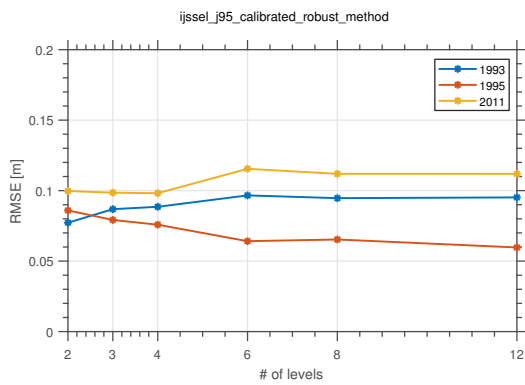


Figure 4.5: RMSE based on the whole discharge wave for 1993, 1995 and 2011 and for varying number of discharge levels based on robust method and 1995 IJssel discharge wave

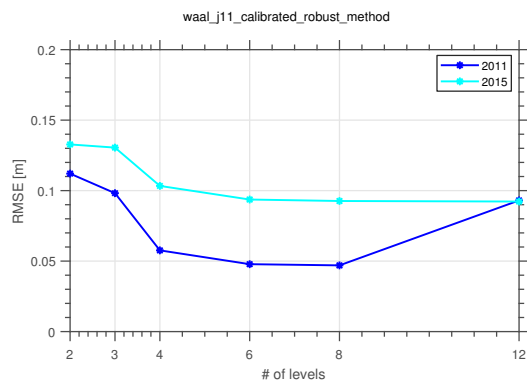


Figure 4.6: RMSE based on the whole discharge wave for 2011 and 2015 and for varying number of discharge levels based on robust method and 2011 Waal discharge wave

5 Discussion

The results show that the calibrated main channel roughness is more sensitive to discharge than location. Even when a varying number of roughness trajectories and a varying number of discharge levels is combined and calibrated, the calibrated roughness is still more sensitive to discharge than location (see Appendix D). Because the modelled summer dike has a large effect on the calibrated roughness in the discharge dependent calibrations, more case studies should be performed on rivers where no summer dike is present. The modelled summer dike option is a specific feature of the models and the SOBEK 3 modelling program. Other modelling programs like HEC-RAS and MIKE lack this feature. The results obtained from the used models are therefore very case-specific.

Another important notion is that the used models are obtained using the WAQ2PROF method. This method generates a 1D model based on 2D model results. Although this indeed generates a quite well performing model, it does not reflect the real situation perfectly. For example, the main channel roughness section widths are underestimated and the resulting flow and total area for the modelled summer dike are physically incorrect. In the first case the floodplain roughness is already affecting the compound roughness when the water is only flowing through the main channel. In the second case the SOBEK modelling program does not account for this unrealistic difference and ignores it. The flow area behind the summer dike is, therefore, overestimated which leads to a higher calibrated roughness than in the situation where the flow area is limited to the total area. Solving these small problems in the WAQ2PROF method or in the new FM2PROF method could lead to generated 1D models from 2D with improved accuracy of the water level predictions.

Furthermore, this study is limited because of the available amount of data. Although much more observation data is available for this study than in a typical calibration study, still more observation data is needed along the longitudinal direction of the river to find an optimum number of roughness trajectories. We used a maximum of seven observation stations to calibrate upon which resulted in a possible maximum number of six roughness trajectories in both Waal and IJssel. The validation showed no actual optimum in the number of roughness trajectories. Still, it would be interesting to know whether an optimum of number of roughness trajectories actually exists beyond this maximum of five roughness trajectories.

Moreover, the calibrated roughness of roughness trajectory TielWaal-Zaltbommel (between 901 and 933 km) shows in all Waal model calibrations a significantly higher roughness. The RMSE values for only observation station TielWaal are also higher than the other observation stations. Preliminary comparisons between these models only showed a bigger difference in bed level around TielWaal because of the use of singlebeam bed level measurements in 1995 opposed to multibeam bed level measurements in 2011. However, this still does not explain why the calibrated roughness at trajectory TW-ZB is significantly higher. A possible explanation is the positioning of the observation station TielWaal. This observation station is located near the Prins Bernardsluizen and not in the main channel of the Waal as is the case with the other observation stations. It is advised to further investigate why the higher roughness at TielWaal occurs.

6 Conclusion and recommendations

6.1 Conclusions

In this study we investigated the location and discharge dependency on the main channel roughness of the River Waal and IJssel by calibration. The roughness is determined by calibrating the Manning coefficient of the main channel in the 1D hydrodynamic models of the River Waal for the winters of 1995 and 2011 and IJssel for the winter of 1995 in the Netherlands. The dependency of the location in the longitudinal direction of the river is modelled using a varying number of roughness trajectories. The discharge dependency is modelled using a varying number of discharge levels.

Results show that the calibrated roughness is mainly sensitive to discharge. At lower discharges the roughness increases as river dunes grow. After this increase the calibrated roughness decreases because of the transition from bankfull to flood stage. At higher discharges the effect of the modelled summer dike becomes dominant resulting in a peak in the calibrated roughness-discharge functions. Including these three features in the calibration method results in more accurate water level predictions. The optimum number of discharge levels ranges between four and eight discharge levels.

Results of the location dependent calibrated roughness show that incorrect boundary conditions and the modelling of bank overflow in sharp bends greatly influence the roughness. For the Waal, two is the optimum found number of roughness trajectories. For the IJssel, three is the optimum found number of roughness trajectories. These optima correspond to an average roughness trajectory length of 40 to 45 km. However, predictions still slightly improve when increasing the number of roughness trajectories in both cases.

6.2 Recommendations

The following recommendations are proposed to further study:

1. The calibrated roughness and the calculated RMSE values near/at observation station TielWaal are different from the rest of the observation stations without a clear explanation. Further study into this difference is advised as it could be a hint of a possible model error.
2. It is recommended to extend this study to other rivers where no summer dike is present. The modelled summer dike in the used models are a specific model feature and is only facilitated by the SOBEK 3 1D hydrodynamic modelling program. It affects the calibrated roughness largely resulting a large peak in the calibrated roughness-discharge functions. Doing the same study with other rivers without a summer dike will result in a more realistic roughness-discharge function. The form of this function could help in aid in the development of 1D hydrodynamic models where the bed roughness is dependent on bed forms.
3. Although this study has used two Dutch rivers of which much more observation data is available than a typical river, still no optimum number of roughness trajectories could be found. It would be interesting to know whether this optimum actually exists. A future study with a river with even more observation data or creating an artificial but representative river in a flume are suggested.

Bibliography

- Bates, P., Horritt, M., Aronica, G., & Beven, K. (2004). Bayesian updating of flood inundation likelihoods conditioned on flood extent data. *Hydrological Processes*, 18(17), 3347–3370. doi:10.1002/hyp.1499
- Berends, K. (2013). *Bijlagen Rijnmodellen 5e generatie SOBEK*. Deltares. Delft.
- Chow, V. (1959). *Open-channel Hydraulics*. McGraw-Hill Book Company. Retrieved from <http://linkinghub.elsevier.com/retrieve/pii/B9780750668576X50000>
- Deltares. (2015). *SOBEK 3 Technical Reference Manual v3.0.1*. Deltares. Delft.
- Hall, J., Tarantola, S., Bates, P., & Horritt, M. (2005). Distributed Sensitivity Analysis of Flood Inundation Model Calibration. *Journal of Hydraulic Engineering*, 131(2), 117–126. doi:10.1061/(ASCE)0733-9429(2005)131:2(117)
- Huthoff, F. & Augustijn, D. (2004). Channel roughness in 1D steady uniform flow: Manning or Chézy? In *Proceedings ncr-days 2004* (pp. 98–100). Retrieved from <http://doc.utwente.nl/59985/>
- Izenman, A. (1991). Recent developments in nonparametric density estimation. *Journal of the American Statistical Association*, 86(413), 205–224. doi:10.1080/01621459.1991.10475021
- Julien, P. (2002). *River Mechanics*. Cambridge University Press.
- Julien, P., Klaassen, G., Ten Brinke, W., & Wilbers, A. (2002). Case Study: Bed Resistance of Rhine River during 1998 Flood. *Journal of Hydraulic Engineering*, 128(12), 1042–1050. doi:10.1061/(ASCE)0733-9429(2002)128:12(1042)
- Mulder, D. (2014). *Applying data-assimilation and calibration in the field of urban drainage* (Doctoral dissertation).
- OpenDA. (2015). *OpenDA User Documentation*.
- Pappenberger, F., Beven, K., Horritt, M., & Blazkova, S. (2005). Uncertainty in the calibration of effective roughness parameters in HEC-RAS using inundation and downstream level observations. *Journal of Hydrology*, 302(1-4), 46–69. doi:10.1016/j.jhydrol.2004.06.036
- Post, J. (2012). *Combining field observations and hydrodynamic models in urban drainage* (Doctoral dissertation).
- Ralston, M. & Jennrich, R. (1978). Dud, A Derivative-Free Algorithm for Nonlinear Least Squares. *Technometrics*, 20(1), 7–14. Retrieved from <http://www.jstor.org/stable/1268154>
- Refsgaard, J., van der Keur, P., Nilsson, B., Müller-Wohlfeil, D.-I., & Brown, J. (2006). Uncertainties in river basin data at various support scales ? Example from Odense Pilot River Basin. *Hydrology and Earth System Sciences Discussions*, 3(4), 1943–1985. Retrieved from <https://hal.archives-ouvertes.fr/hal-00298743>
- Schwanenberg, D., van Breukelen, A., & Hummel, S. (2011). Data assimilation for supporting optimum control in large-scale river networks. In *2011 international conference on networking, sensing and control* (pp. 98–103). IEEE. doi:10.1109/ICNSC.2011.5874881
- Vidal, J.-P., Moisan, S., Faure, J.-B., & Dartus, D. (2007). River model calibration, from guidelines to operational support tools. *Environmental Modelling & Software*, 22(11), 1628–1640. doi:10.1016/j.envsoft.2006.12.003
- Warmink, J. (2011). *Unraveling uncertainties* (Doctoral dissertation, University of Twente, Enschede, The Netherlands). doi:10.3990/1.9789036532273
- Warmink, J., Booij, M., van der Klis, H., & Hulscher, S. (2007). Uncertainty in water level predictions due to various calibrations. In *Caiwa* (pp. 1–18).
- Warmink, J., van der Klis, H., Booij, M., & Hulscher, S. (2011). Identification and Quantification of Uncertainties in a Hydrodynamic River Model Using Expert Opinions. *Water Resources Management*, 25(2), 601–622. doi:10.1007/s11269-010-9716-7
- Wilbers, A. & Ten Brinke, W. (2003). The response of subaqueous dunes to floods in sand and gravel bed reaches of the Dutch Rhine. *Sedimentology*, 50(6), 1013–1034. doi:10.1046/j.1365-3091.2003.00585.x

A Method for modelling armoured bed layers and submerged groynes

The roughness of the armoured bed layers and submerged groynes is different from the surrounding river bed and should be taken into account in the calibration. A description of how to model these layers is documented in Berends, 2013. In summary, a factor α is determined using the roughness results of a 2D hydrodynamic model for several discharge levels by dividing the roughness at the layer by the roughness upstream of the layer. The roughness of the different bed layer can then be calculated using $n_{layer} = \frac{\alpha}{n_{normal}}$ (Manning). For each discharge wave and layer location the alpha values will differ and therefore need to be determined for each different discharge wave and location.

A.1 1995 - Armoured bed layer Nijmegen

In 1995 only the armoured bed layer near Nijmegen was operational. Figure A.1 shows the discharge- α relation for the armoured bed layer at Nijmegen for 1995.

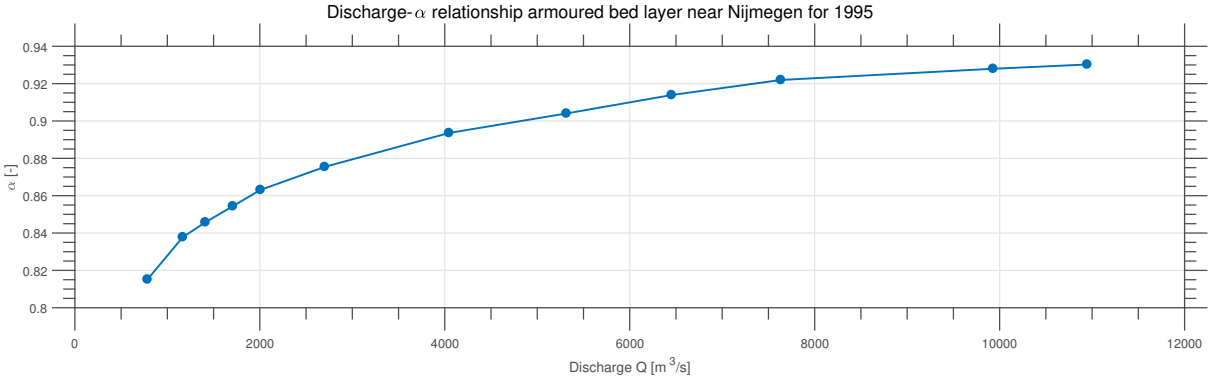


Figure A.1: Discharge- α relationship for the armoured bed layer at Nijmegen for 1995

A.1.1 2011 - Armoured bed layers Nijmegen and Sint Andries and submerged groynes Erlecom

In 2011 both armoured bed layers (Nijmegen and Sint Andries) and submerged groynes (Erlecom) were operational. Figure A.2 presents the discharge- α relationship for the three different layers for 2011.

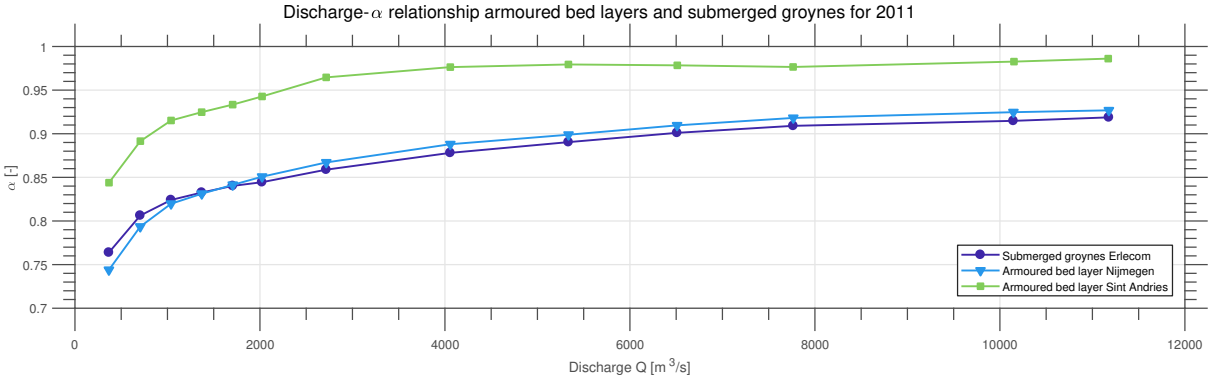


Figure A.2: Discharge- α relationship for the armoured bed layers at Nijmegen and Sint Andries and for the submerged groynes at Erlecom for 2011

B Water level frequency distributions

Figure B.1 illustrates the water level frequency distributions at the four observation stations of the Waal (i.e. Nijmegenhaven, TielWaal, Zaltbommel and Vuren) used in the RMSE calculation. Figure B.2 presents the distributions for the IJssel. The discharge waves of 1993 and 1995 show a long lower tail at the higher water levels, indicating that lower water levels are more frequent than higher ones. The water level distributions of 2011 and 2015 are more Gaussian like.

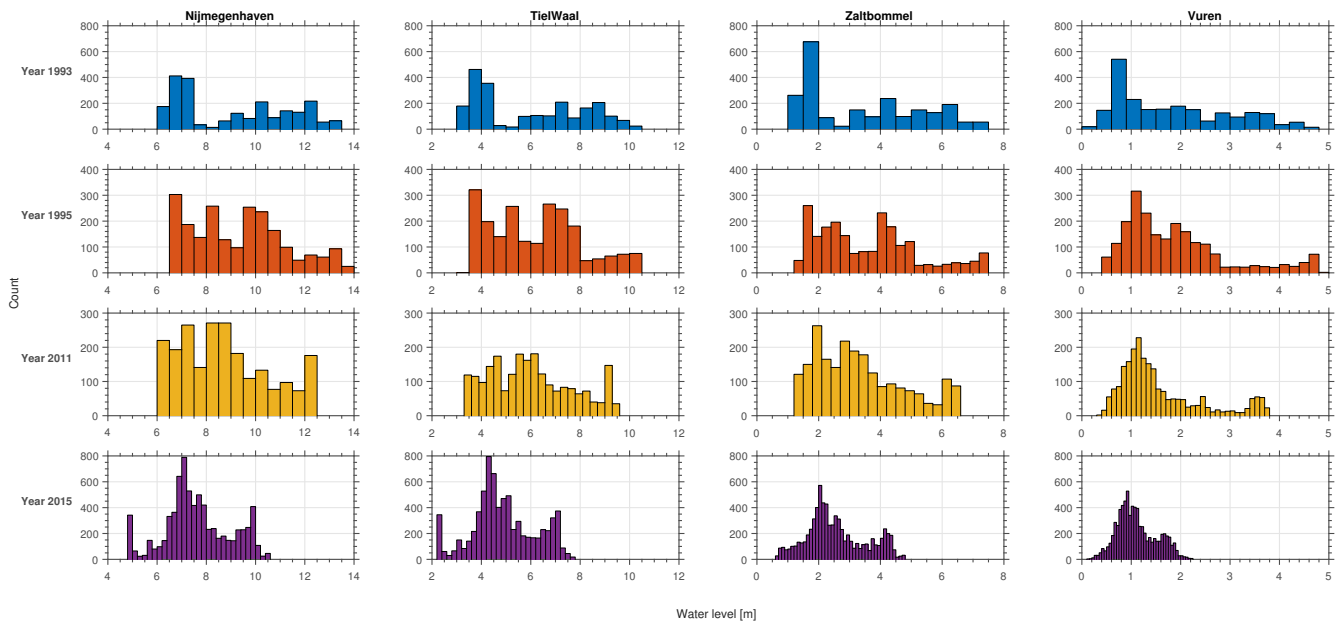


Figure B.1: Waterlevel frequency distributions at observation stations Nijmegenhaven, TielWaal, Zaltbommel and Vuren in the Waal using bin size based on Freedman-Diaconis rule for discharge waves of 1993, 1995, 2011 and 2015

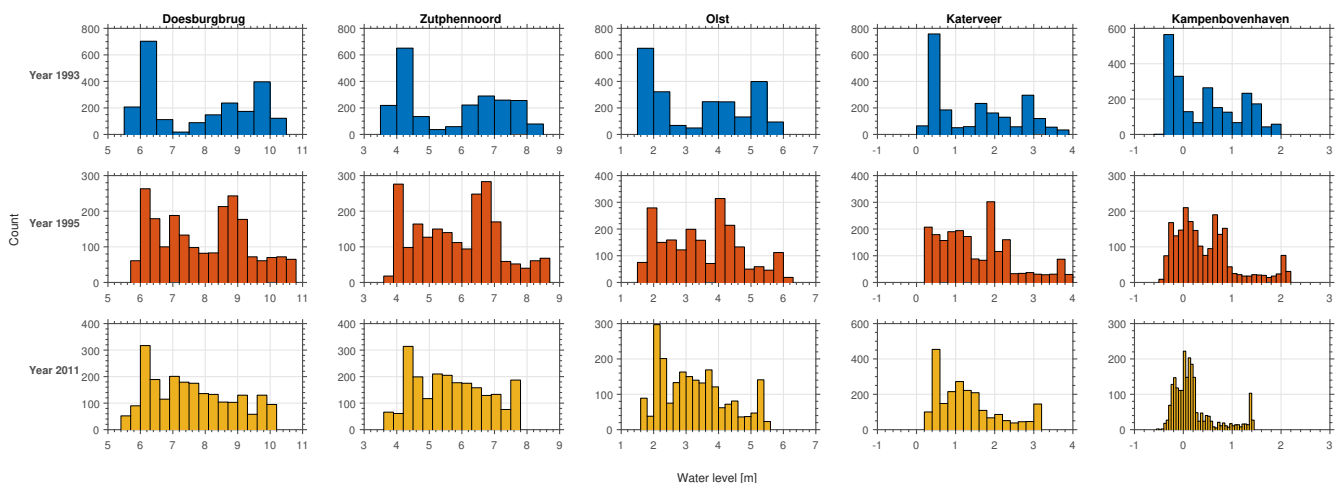


Figure B.2: Waterlevel frequency distributions at observation stations Doesburgbrug, Zutphennoord, Olst, Katerveer, Kampenbovenhaven in the IJssel using bin size based on Freedman-Diaconis rule for discharge waves of 1993, 1995 and 2011

C Calibrated roughness for discharge dependency for Waal 1995 - scenario 1, 2 and 3

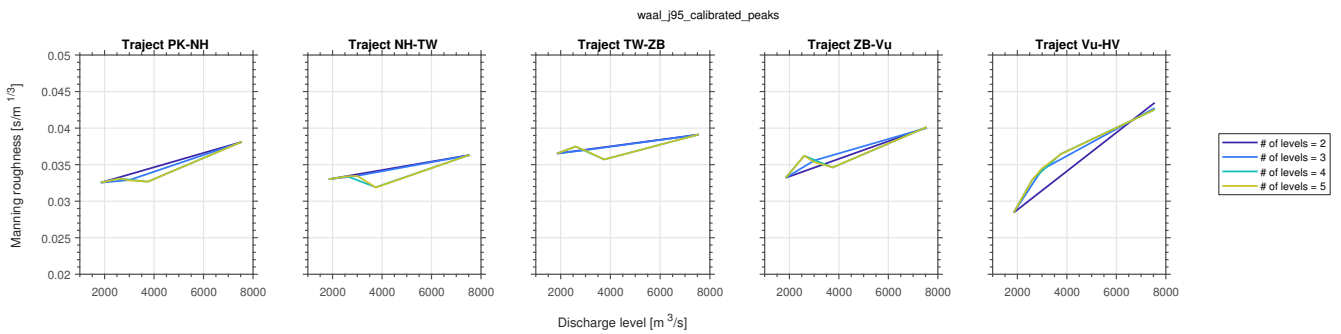


Figure C.1: Calibrated roughness-discharge functions of the Waal for 1995 discharge wave for varying number of discharge levels based on peaks (scenario 1)

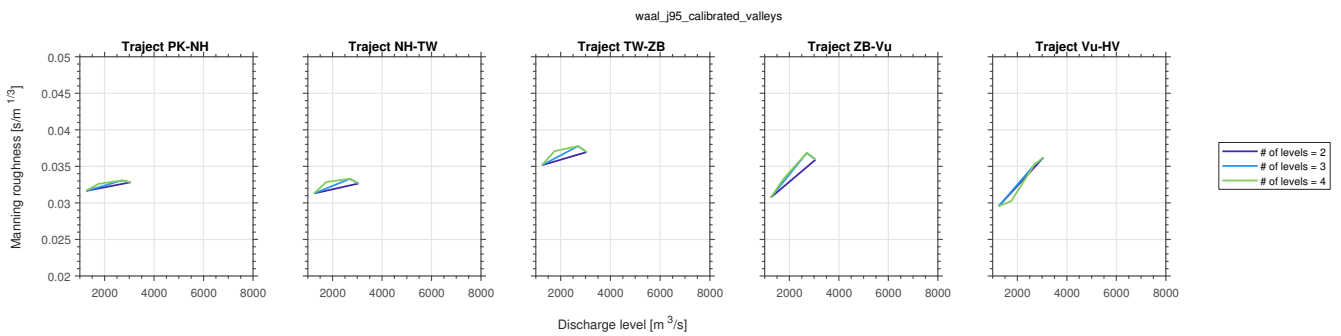


Figure C.2: Calibrated roughness-discharge functions of the Waal for 1995 discharge wave for varying number of discharge levels based on valleys (scenario 2)

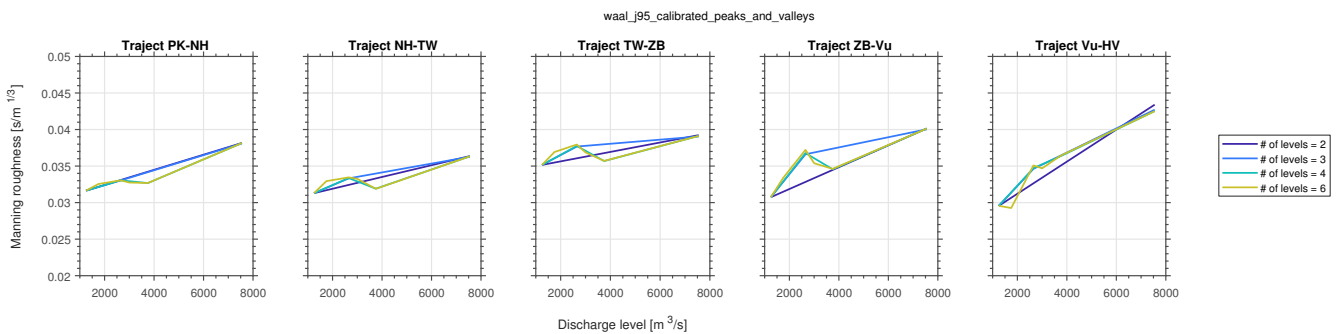


Figure C.3: Calibrated roughness-discharge functions of the Waal for 1995 discharge wave for varying number of discharge levels based on peaks and valleys (scenario 3)

D Validation location and discharge dependency combined for Waal 1995

Figure D.1 presents the accuracy of water level predictions for the Waal 1995 calibration expressed using the adapted RMSE criterion when both the location and discharge dependency are combined. It clearly shows the accuracy of water level predictions (and thus roughness) is mostly dependent on the discharge as expected from the non-combined results.

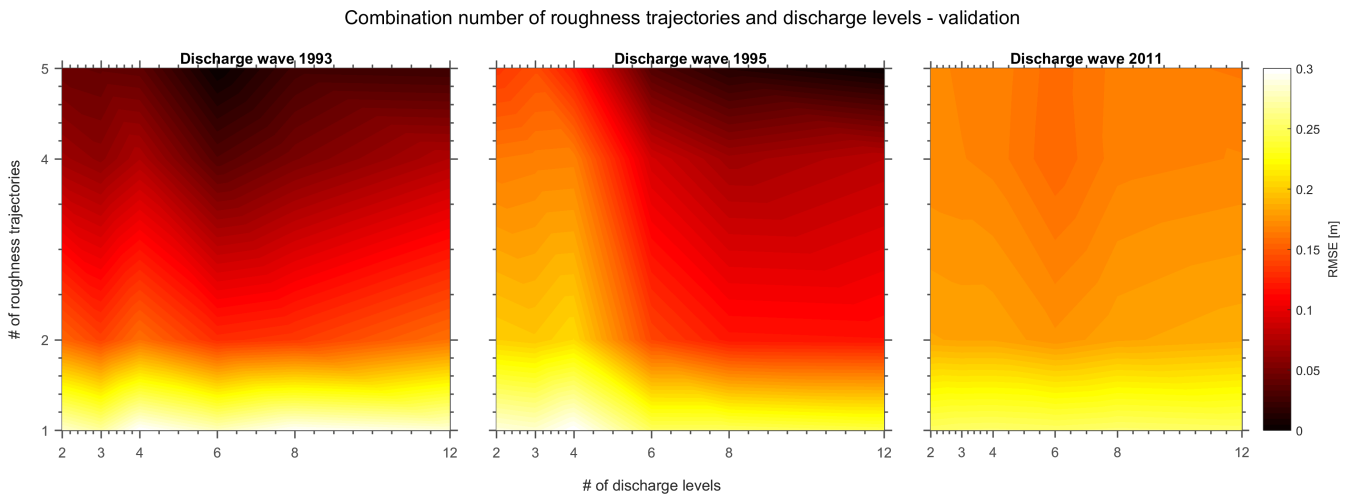


Figure D.1: Model performance when both location and discharge dependency are combined. Location dependency is based on the roughness trajectory configuration described in section 3 of the method. Discharge dependency is based on the robust method

E 2D WAQUA 1995 Waal calibration results

As an addition to the 1D calibration results, a calibration with the 2D WAQUA 1995 Waal model is performed using the five existing roughness trajectories and six discharge levels based on the robust method. In this calibration the α -value in a simplified version of the Van Rijn roughness height predictor is calibrated. The sections below present the result of this calibration with a comparison to the calibrated roughness obtained for the 5th generation of the Rhine model.

E.1 Calibrated roughness

Figure E.1 presents the calibrated roughness α -value of the 2D WAQUA 1995 Waal model for the five existing roughness trajectories and six discharge levels based on the robust method and the original calibrated roughness of the 5th generation. The figure clearly shows different discharge-roughness functions but they share two features, namely the roughness increases at low discharge but decreases slightly at high discharge. The roughness increase can be attributed to growth of river dunes. The roughness decrease is a possible consequence of the simplified Van Rijn roughness height predictor or the White-Colebrook roughness formula. However, these conclusions are not thoroughly tested and should be further investigated. The transition from bankfull to flood stage and the effect of the modelled summer dike as found in the 1D model calibration cases is not present in these calibrated roughness-discharge functions, because the transition and the summer dike is more accurately modelled in 2D. Overall the roughness increases in the figure for increasing discharge which is what we expect from river dune growth. However, more research on this topic is needed as the results are very preliminary.

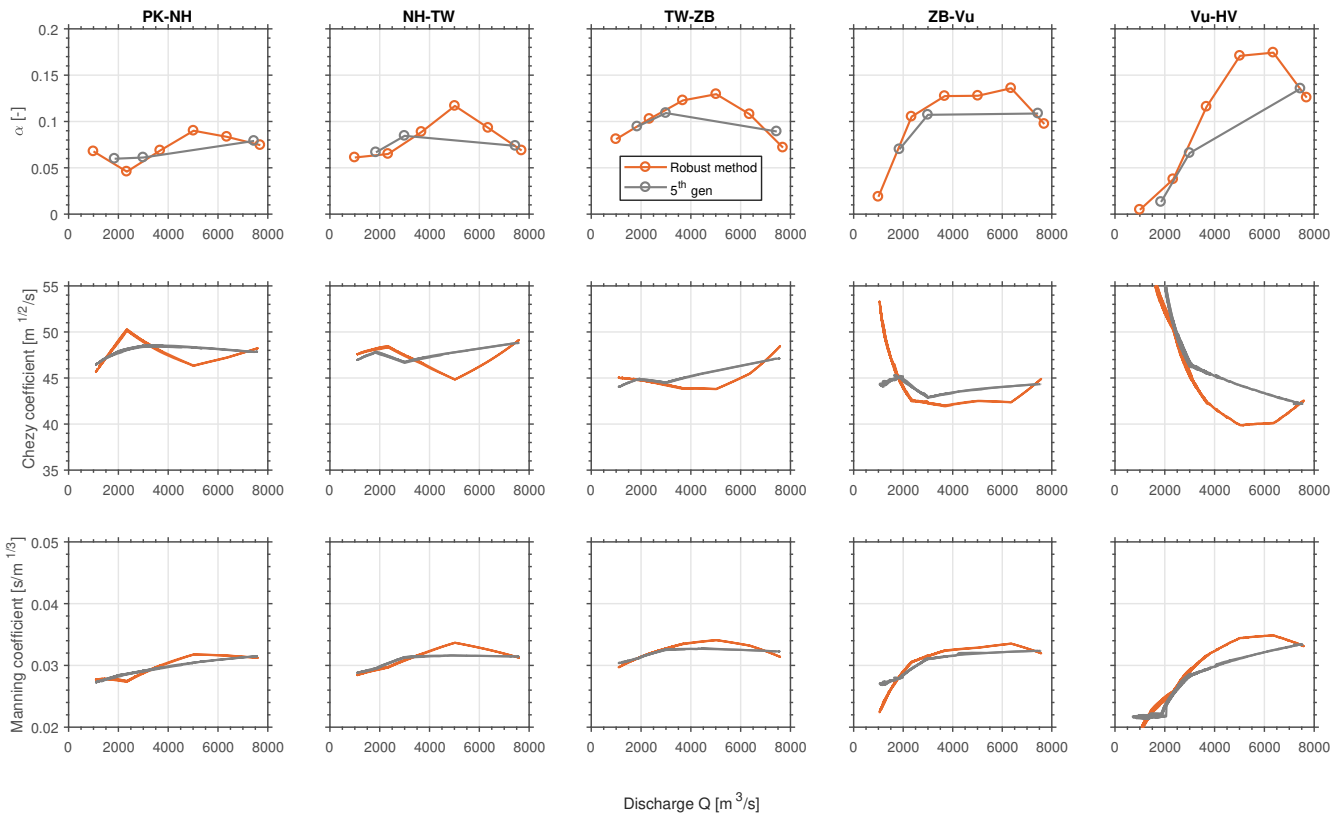


Figure E.1: Calibrated roughness of the 2D WAQUA 1995 Waal model for the five existing roughness trajectories and six discharge levels based on the robust method and the original calibrated roughness of the 5th generation. The conversion to Chezy and Manning values is based on the model results (i.e. discharge and water depth)

E.2 Model performance

Table E.1 presents the difference in model performance between the new robust method and 5th generation calibrated roughness cases. The comparison shows that the robust method with six discharge levels improves the overall model performance compared to the 5th generation.

Table E.1: Difference in model performance between the new robust method and 5th generation calibrated roughness cases. Lower MAE (mean absolute error) and RMSE (root mean square error) and negative differences mean better overall model performance

		1995 (calibration)			
		Nijmegenhaven	TielWaal	Zaltbommel	Vuren
5th gen	MAE	0.062	0.054	0.083	0.046
	RMSE	0.090	0.105	0.142	0.130
Robust method	MAE	0.043	0.038	0.040	0.029
	RMSE	0.056	0.051	0.055	0.040
Difference	MAE	-30.7%	-30.8%	-52.4%	-37.4%
	RMSE	-38.6%	-51.2%	-60.8%	-69.5%
		1993 (validation)			
		Nijmegenhaven	TielWaal	Zaltbommel	Vuren
5th gen	MAE	0.061	0.075	0.106	0.051
	RMSE	0.108	0.117	0.143	0.103
Robust method	MAE	0.076	0.084	0.046	0.035
	RMSE	0.106	0.112	0.099	0.070
Difference	MAE	24.4%	12.4%	-56.5%	-30.9%
	RMSE	-1.9%	-4.7%	-30.7%	-31.9%
		2011 (validation)			
		Nijmegenhaven	TielWaal	Zaltbommel	Vuren
5th gen	MAE	0.061	0.194	0.175	0.060
	RMSE	0.082	0.214	0.210	0.125
Robust method	MAE	0.052	0.172	0.120	0.036
	RMSE	0.069	0.185	0.147	0.062
Difference	MAE	-15.7%	-11.5%	-31.5%	-40.8%
	RMSE	-15.0%	-13.4%	-30.1%	-50.2%